Biomechanical Responses to Synthetic and Natural Turf during Locomotion

by

Brandi Elizabeth Decoux

A dissertation submitted to the Graduate Faculty of
Auburn University
in partial fulfillment of the
requirements for the Degree of
Doctor of Philosophy

Auburn, Alabama
August 3, 2019

Keywords: biomechanics, stiffness, coordination variability, running, hopping, turf

Approved by

Wendi H. Weimar, Chair, Professor of Kinesiology
Nels H. Madsen, Professor Emeritus of Mechanical Engineering
Gretchen D. Oliver, Professor of Kinesiology
J. Scott McElroy, Professor of Crop, Soil and Environmental Sciences.
Danielle D. Wadsworth, Associate Professor of Kinesiology
Jaimie A. Roper, Assistant Professor of Kinesiology

Abstract

The ability of athletes to adapt their movement patterns appropriately to varying constraints imposed by the playing environment is crucial for performance as well as musculoskeletal health. For outdoor athletes, playing environment variations are often derived from synthetic and natural turf surfaces. The purpose of this project was to assess biomechanical movement parameters of hopping and running on four different turf surfaces—three synthetic and one natural—through two separate specific aims. For the first aim, vertical and leg stiffness and movement frequencies were analyzed during these movements to determine whether athletes interpret differences between synthetic and natural turf surfaces. No differences between surfaces were not found, indicating that the body interprets the demands of the tested surfaces to be similar. For the second aim, inter-segmental coordination variability between six segment couplings was examined during the braking and propulsion sub-phases of running and hopping to determine whether synthetic and natural turf surfaces affect how athletes regulate the lower extremity linked-segment system. Only one difference in coordination variability was detected. Specifically a reduction in coordination variability in the pelvis-thigh sagittal plane coupling during the braking phase of hopping was observed on the firmest of the synthetic turf surfaces compared to the natural. Overall, the consistency in the biomechanical responses to these surfaces during running and hopping suggest that the musculoskeletal system does not perceive there to be a need for different movement patterns on synthetic and natural turf and warrants further investigation.

Acknowledgments

To my family—I would never have made it this far without each one of you. I cannot thank you enough for your unconditional love, support, and encouragement. This is for you.

List of Tables

Table 2.1: Summary of cited studies pertaining athletic performance and continuous relative phase coordination variability 16

Table 2.2: Summary of cited studies pertaining injury and continuous relative phase coordination variability 19

Table 3.1: Turf System Specifications of Each Testing Surface 26

Table 4.1: Turf System Specifications of Each Testing Surface 43

Table 4.2: Stiffness and frequency parameters of hopping and running 52

Table 5.1: Turf System Specifications of Each Testing Surface 58

Table 5.2: Continuous relative phase (CRP) variability during the braking and propulsion sub-phases of hopping 70

Table 5.3: Continuous relative phase (CRP) variability during the braking and propulsion sub-phases of running 71

List of Figures

Figure 3.1: Cleat models used in this study 28

Figure 3.2: IMU sensor placement............ 29

Figure 3.3: Phases, sub-phases, and key events of hopping 31

Figure 3.4: Phases, sub-phases, and key events of running............ 32

Figure 3.5: Concurrent timing of peak vertical ground reaction force and maximum vertical center of mass displacement during hopping and running............ 33

Figure 3.6: Absolute segment angles computed relative to the global sagittal and frontal planes............ 36

Figure 4.1: Cleat models used in this study 44

Figure 4.2: IMU sensor placement............ 45

Figure 4.3: Phases, sub-phases, and key events of hopping 47

Figure 4.4: Phases, sub-phases, and key events of running............ 48

Figure 5.1: Cleat models used in this study 60

Figure 5.2: IMU sensor placement............ 61

Figure 5.3: Phases, sub-phases, and key events of hopping 63

Figure 5.4: Phases, sub-phases, and key events of running............ 64

Figure 5.5: Concurrent timing of peak vertical ground reaction force and maximum vertical center of mass displacement during hopping and running............ 65

Figure 5.6 Absolute segment angles computed relative to the global sagittal and frontal planes............ 66

Table of Contents

Abstract ii

Acknowledgments iii

List of Tables iv

List of Figures v

CHAPTER 1: Introduction 1

    Purpose 3

    Specific Aims 3

    Research Questions and Hypotheses 4

    Limitations 6

    Delimitations 6

    Terms 7

CHAPTER 2: Review of Literature 8

    Stiffness 8

    Coordination Variability 13

    Synthetic and Natural Turf 22

    Summary 23

CHAPTER 3: Methods 25

    Participants 25

    Design and Protocol 27

Data Acquisition and Processing 30

Stiffness Measures 34

Coordination Variability Measures 36

Statistical Analysis 38

CHAPTER 4: Investigation of leg spring behavior during hopping and running on natural and synthetic turf playing surfaces 39

Introduction 39

Methods 42

Participants 42

Design and Protocol 42

Data Acquisition and Processing 46

Statistical Analysis 51

Results 51

Discussion 53

Conclusion 54

CHAPTER 5: Inter-segmental coordination variability during hopping and running on natural and synthetic turf surfaces 55

Introduction 55

Methods 57

Participants 57

Design and Protocol 59

Data Acquisition and Processing 62

Statistical Analysis 68

Results 68

Discussion 69

Conclusion 72

REFERENCES 73

APPENDIX 89

CHAPTER I

Introduction

Athletes are tasked with performing and adapting to varying environmental demands, some of which are directly related to the surface properties on which they are performing (Ferris, Louie, & Farley, 1998; Kerdok, Biewener, McMahon, Weyand, & Herr, 2002; Nigg and Yeadon, 1987). In particular, athletes who perform on synthetic and natural turf surfaces must appropriately interpret and respond to these surfaces with a variety of movement solutions (Seifert, Button, & Davids, 2013). By regulating contributions from the components of the musculoskeletal system and exploiting the abundant degrees of freedom within the body, skilled athletes exhibit a range of movement solutions to adapt to changes in turf surfaces with different properties, such as stiffness and traction. Adaptability in this context is vital for performance parameters to be minimally effected and injury risks to be mitigated (Hamill, Palmer, & Van Emmerik, 2012; Seifert, et al., 2013).

Two biomechanical perspectives from which movement adaptions are often examined, were adopted in this project. The first approach simplifies the bouncing movement of the body during hopping and running using the mass-spring model. In this model, the body's center of mass serves as a point mass that is supported by a massless spring (Blickhan, 1989; Farley, Blickhan, Saito, & Taylor, 1991; Farley, Blickhan, & Taylor, 1985; Farley and Gonzalez, 1996; McMahon and Cheng, 1990). The behavior of the spring is characterized by its resistance to deformation under an applied load which is known at stiffness (Blickhan, 1989; McMahon and

Cheng, 1990). During submaximal locomotion such as hopping and running, leg stiffness, which refers to the resistance to change in leg length when a force is applied (Blum, Lipfert, & Seyfarth, 2009; Brughelli and Cronin, 2008; Butler, et al., 2003; Serpell, et al., 2012), has been shown to be effectively adjusted in response to the surface stiffness, so that the total stiffness of the spring and the surface is maintained (Farley, Houdijk, Van Strien, & Louie, 1998; Ferris and Farley, 1997; Ferris, et al., 1998). Total stiffness in this context is represented by a measure called vertical stiffness. This measure encompasses deformation of both the leg spring and the surface and is calculated as the ratio of vertical center of mass displacement to the maximum vertical force applied to the system (Ferris and Farley, 1997; Ferris, et al., 1998). Similar strategies have also been observed on even more compliant surfaces and on uneven surfaces (Ferris, Liang, & Farley, 1999; Karamanidis, Arampatzis, & Brüggemann, 2006; Kerdok, et al., 2002). These findings suggest that the body will exploit the adjustable stiffness properties of the lower extremity to respond to different surfaces in order to maintain center of mass dynamics (Marigold and Patla, 2005).

The second approach implemented to explore locomotor adaptations on synthetic and natural turf focuses on the response of pairs segments within the same limb. As opposed to stiffness, which represents a simplified, composite measure of the contributions of the musculoskeletal system to lower extremity movement, inter-segmental coordination variability gives attention to the process of coordinating intralimb contributions of relative segments within the same limb in response to changes in environmental demands (Davids, Glazier, Araujo, & Bartlett, 2003; Newell, 1986). A certain range of coordination variability is considered to be necessary for carrying out movements with high efficacy and efficiency in addition to being indicators of healthy and functional coordination dynamics (Hamill, Haddad, Heiderscheit, Van

Emmerik, & Li, 2006; Stergiou and Decker, 2011). However observations of a reduction in variability may place that system at greater risk of injury due to repetitive stress being applied to the same tissues (Hamill, van Emmerik, Heiderscheit, & Li, 1999).

The ability to adapt lower extremity stiffness and coordination variability is essential for meeting a range movement constraints in a dynamic environment, especially for athletes tasked with playing of different surfaces like synthetic and natural turf. As the number of synthetic turf fields continues to grow, the need for understanding how these surfaces influence injury and performance also grows. While developments in synthetic turf have helped to reduce dissimilarities between synthetic turf and natural turf, differences in key physical properties such as surface stiffness still exist (Fleming, 2011; Severn, Fleming, & Dixon, 2008). By investigating stiffness and coordination variability on different synthetic turf surfaces and natural turf, much needed insight on how the body interprets and responds to the stiffness of these surfaces can be gained. This information is valuable for athletes preparing to compete on these surfaces as well as turf manufacturers concerned with athlete performance and safety.

Purpose

The purpose of this project was to investigate lower limb spring behavior, coordination on three different types of synthetic turf surfaces and one natural turf surface.

Specific Aims

Aim 1: To determine whether athletes interpret differences in synthetic and natural turf surfaces by investigating vertical stiffness, leg stiffness, and self-selected frequency during hopping and running.

Aim 2: To determine whether synthetic and natural turf surfaces affect how athletes regulate the linked-segment system of the lower extremity by investigating inter-segmental coordination variability during two fundamental sport-related tasks, hopping and running,

Research Questions and Hypotheses

Aim 1

RQ 1.1: Does vertical stiffness during hopping differ between synthetic and natural turf?

Hypothesis: Vertical stiffness during hopping would not differ between turf surfaces.

RQ1.2: Does vertical stiffness during running differ between synthetic and natural turf?

Hypothesis: Vertical stiffness during running would not differ between turf surfaces.

RQ 1.3: Does leg stiffness during hopping differ between synthetic and natural turf?

Hypothesis: Leg stiffness during hopping would be greatest on natural turf and progressively less on synthetic turf 3, synthetic turf 2, and synthetic turf 1, respectively.

RQ 1.4: Does leg stiffness during running differ between synthetic and natural turf?

Hypothesis: Leg stiffness during running would be greatest on natural turf and progressively less on synthetic turf 3, synthetic turf 2, and synthetic turf 1, respectively.

RQ 1.5: Does self-selected hopping frequency differ between synthetic and natural turf?

Hypothesis: Self-selected hopping frequency would not differ between turf surfaces.

RQ 1.6: Does self-selected stride frequency differ between synthetic and natural turf?

Hypothesis: Self-selected stride frequency would not differ turf surfaces.

Aim 2

RQ 2.1: Does inter-segmental coordination variability during the braking sub-phase of hopping differ between synthetic and natural turf?

Hypothesis: Inter-segmental coordination variability during the braking sub-phase of hopping would be greatest on natural turf and progressively reduced on synthetic turf 3, synthetic turf 2, and synthetic turf 1, respectively.

RQ 2.2: Does inter-segmental coordination variability during the propulsion sub-phase of hopping differ between synthetic and natural turf?

Hypothesis: Inter-segmental coordination variability during the propulsion sub-phase of hopping would be greatest on natural turf and progressively reduced on synthetic turf 3, synthetic turf 2, and synthetic turf 1, respectively.

RQ 2.3: Does inter-segmental coordination variability during the braking sub-phase of running differ between synthetic and natural turf?

Hypothesis: Inter-segmental coordination variability during the braking sub-phase of running would be greatest on natural turf and progressively reduced on synthetic turf 3, synthetic turf 2, and synthetic turf 1, respectively.

RQ 2.4: Does inter-segmental coordination variability during the propulsion sub-phase of running differ between synthetic and natural turf?

Hypothesis: Inter-segmental coordination variability during the propulsion sub-phase of running would be greatest on natural turf and progressively reduced on synthetic turf 3, synthetic turf 2, and synthetic turf 1, respectively.

Limitations

The following limitations are acknowledged:

1. The athletic background of participants varied.
2. Surface and ambient temperature were not controlled.
3. Peak ground reaction force was modeled and not measured directly.

Delimitations

Delimitation of this project are as follows:

1. All participants were males.

2. Individuals who had undergone surgery to their lower extremity but were cleared by a physician as fully recovered were not included in this study.
3. Only football cleats of two very similar models were used.

Terms

Stiffness — Ratio of load to deformation caused by that load.

Vertical Stiffness— Ratio of peak vertical ground reaction force to center of mass vertical displacement; represents the total series stiffness of the lower extremity and the surface.

Leg Stiffness — Ratio of peak vertical ground reaction force to change in leg length from standing length to the maximum shortened length.

Coordination Dynamics — The mechanisms and parameters by which the many degrees of freedom of the musculoskeletal system are regulated to generate functionally adaptive yet stable movements

CHAPTER 2

Review of Literature

The purpose of this project was to investigate the influence of different synthetic and natural turf surfaces on leg and vertical stiffness, movement frequencies, and inter-segmental variability during hopping and running. This chapter is broken into three sections and presents a review of the literature on the main topics of this project. Specifically, stiffness, coordination variability and turf systems will be addressed.

Stiffness

During bouncing movement patterns such as hopping and running, the behavior of the lower extremity supporting the mass of the body can be represented at a simple linear spring (Blickhan, 1989). Integrated contributions of the musculoskeletal system act to resist applied loads and store and return mechanical energy during ground contact. This response is described with a mechanical measure of spring behavior called stiffness. According to Hooke's law, stiffness is a characteristic of a linear spring describing its resistance to deformation when a force is applied (Blickhan, 1989; McMahon and Greene, 1979). Biomechanically, the body resists deformation through anatomical and neurological controls.

Stiffness during bouncing gaits can be considered the combined efforts of ligaments, tendons, bones, muscles, and other musculoskeletal elements of the lower extremity linked-segment system, working to control center of mass movement (Kerdok, et al., 2002; McMahon and Cheng, 1990). However, stiffness is typically used in the literature to simplify the lower extremity dynamics into an intuitive representative measure. Depending on the research focus, different measures of stiffness have been used throughout the literature to characterize the behavior of spring systems, particularly during the contact phase of running and hopping. The two most common measures studied are vertical stiffness and leg stiffness.

Vertical stiffness is the most comprehensive of the measures as it refers to a system's combined resistance to vertical displacement of the center of mass after a vertical force is applied (Brughelli and Cronin, 2008; Buchheit, Gray, & Morin, 2015; Butler, Crowell III, & Davis, 2003; Farley, et al., 1985; McMahon and Cheng, 1990; Serpell, Ball, Scarvell, & Smith, 2012). It is calculated as the ratio of peak vertical ground reaction force (GRF) to vertical displacement of the center of mass (Farley, et al., 1985; McMahon and Cheng, 1990; Serpell, et al., 2012). In most research analyzing vertical stiffness, this measure represents the linear spring behavior of the body in the vertical direction (Brughelli and Cronin, 2008; Butler, et al., 2003). However in studies investigating the influence of compliant surface stiffness on the leg spring (Farley, et al., 1998; Ferris and Farley, 1997; Ferris, et al., 1999; Ferris, et al., 1998; Kerdok, et al., 2002; Moritz and Farley, 2004), vertical stiffness actually represents the combined series stiffness of both the leg and the surface in the vertical direction since center of mass displacement in this context occurs due to leg spring compression (i.e., flexion at the joints of the lower extremity) as well as the surface deformation (Ferris and Farley, 1997; Serpell, et al., 2012). Thus, the value of vertical stiffness is that it presents a measure that consolidates the influence of the deformation from the two interacting systems. However, by taking both the system and the surface deformation into consideration, the response of the leg specifically is masked.

In order to characterize the behavior of the leg apart from the surface, leg stiffness must be assessed. Leg stiffness refers to the resistance to change in leg length when a force is applied (Blum, Lipfert, & Seyfarth, 2009; Brughelli and Cronin, 2008; Butler, et al., 2003; Serpell, et al., 2012). It is calculated as the ratio of peak GRF to change in leg length. When measured during vertical hopping and jumping tasks on firm surfaces, vertical and leg stiffness are equivalent because center of mass displacement occurs solely as a function of leg compression (McMahon and Cheng, 1990). However, in horizontal locomotion, leg stiffness is dependent on additional factors including horizontal velocity and approach angle at contact (Brughelli and Cronin, 2008). Leg and vertical stiffness therefore often provide different information when applied to running (Brughelli and Cronin, 2008; Serpell, et al., 2012).

Athletes are tasked with performing and adapting to varying environmental demands, some of which are directly related to the surface properties on which they are performing (Ferris, et al., 1998; Kerdok, et al., 2002; Nigg and Yeadon, 1987). During hopping and running specifically, adaptations have been observed to take place in the leg spring in response to surfaces of different stiffnesses (Farley, et al., 1998; Ferris and Farley, 1997; Ferris, et al., 1998; Kerdok, et al., 2002). Findings from these studies have revealed the ability of the lower extremity to effectively maintain a constant vertical stiffness by making adjustments in leg stiffness to counter changes in surface stiffness. Adaptations in leg stiffness to maintain vertical stiffness have also been observed on very compliant surfaces that experience noticeable deformation (i.e., foam) as well as on uneven surfaces (Ferris, et al., 1999; Grimmer, Ernst, Günther, & Blickhan, 2008; Karamanidis, et al., 2006; Kerdok, et al., 2002). More recently, a study comparing leg stiffness during hopping on tennis court surfaces that are considered to be on the stiffer end of the spectrum (i.e., acrylic and clay courts), found that tennis players exhibited a practically significant 5% reduction in leg stiffness during on the clay court compared to the acrylic court (Maquirriain, 2013). This finding indicates that tennis players are able to make proper adaptations in leg stiffness on different court surfaces, which the authors suggest is important for maintaining similar movement patterns.

Leg and vertical stiffness control on difference surfaces has also been investigated during interactions with new and unexpected surfaces. For example, Ferris, et al. (1999) found that leg stiffness in runners could be adjusted properly as early as their first step taken on a new surface. They found that runners transitioning from a compliant surface to a stiffer surface maintained the same vertical stiffness during the initial step on the stiff surface as exhibited on the stiffer surface. Furthermore, research by Moritz and Farley (2004) tested the ability of the leg spring to adjust to anticipated and unanticipated changes in surfaces. They found that vertical stiffness was maintained when hopping onto an expected, unexpected, and random hard surface from a soft surface, and leg stiffness was adjusted through passive control mechanisms requiring no neural feedback, including intrinsic force-length properties of the lower extremity muscles and interdependent segment orientations at the knee and hip of the same limb. This finding has valuable implications for athletes that encounter a range of playing surfaces. Particularly, keeping vertical stiffness consistent across different surfaces is considered to be an essential locomotive control strategy for conserving center of mass dynamics and has been suggested to be important for optimizing movement efficiency (Kerdok, et al., 2002; Moritz and Farley, 2004).

It is widely accepted that stiffness plays an important role in various aspects of athletic performance (Brazier et al., 2014; Butler, et al., 2003; Pruyn, Watsford, & Murphy, 2014). In regards to efficiency, research has indicated that optimal levels of stiffness can improve mechanical and metabolic economy (Hunter and Smith, 2007; Kerdok, et al., 2002; McMahon and Cheng, 1990; Slawinski, Heubert, Quievre, Billat, & Hannon, 2008). Additionally, increased stiffness has been shown to enhance energy storage, energy return and even improve the rate of force development (Arampatzis et al., 2006; Latash and Zatsiorsky, 1993; Pruyn, et al., 2014) while decreases in stiffness are important during high impacts with the ground in order to mitigate excessive forces (Devita and Skelly, 1992; Dufek and Bates, 1990; Farley, et al., 1991).

While research related to athletic performance has indicated that leg stiffness can be tuned to suit the task demands, it is important to note that significantly elevated or reduced levels of leg stiffness have implications regarding injury risk. Excessive leg stiffness is believed to increase injury risk to bone tissue due to repetitive loads transmitted through minimally flexed lower extremity joints (Butler, et al., 2003; Williams III, Davis, Scholz, Hamill, & Buchanan, 2004; Williams III, McClay, & Hamill, 2001). Conversely, a lack of stiffness in the leg spring has implications for elevated risk of soft tissue damage (e. g. , muscle strain) as a result of increased muscular demand needed for force attenuation (Butler, et al., 2003; Pickering Rodriguez, Watsford, Bower, & Murphy, 2017; Williams III, et al., 2004; Williams III, et al., 2001; Williams III, Murray, & Powell, 2016).

As the number of synthetic turf fields continues to grow, the need for understanding how these surfaces influence injury and performance also grows. While developments in synthetic turf have helped to reduce dissimilarities between synthetic turf and natural turf, differences in key physical properties such as surface stiffness still exist (Fleming, 2011; Severn, et al., 2008). By investigating vertical and leg stiffness on different synthetic turf surfaces and natural turf, much needed insight on how the body interprets and responds to the stiffness of these surfaces will be gained. This information is valuable for athletes preparing to compete on these surfaces as well as turf manufacturers concerned with athlete performance and safety.

Coordination Variability

Coordination of human movement is a complex element of movement control that takes place amongst a network of hierarchical levels of the body (Diedrichsen, Shadmehr, & Ivry, 2010). In order to carry out coordinated voluntary movement, components of the nervous system, muscular system, and skeletal system, supported by contributions from other biological systems (e.g., respiratory and cardiovascular), work together as an integrated human movement system (A. M. Williams, Davids, & Williams, 1999). The mechanical degrees of freedom referred to originally by Bernstein in his explanation of coordination come from the muscular and skeletal systems (i.e., segments, joints, and muscles)(Bernstein, 1967; van Emmerik, Ducharme, Amado, & Hamill, 2016). When muscles are activated and contract to move or stabilize segments, sensory receptors located within the musculoskeletal system provide feedback to the nervous system about segmental positions and tension parameters in the muscles. These proprioceptive inputs in addition to the perceptual and tactile sensory input gathered from the environment-performer interaction and information about the involved environmental, organismic, and task constraints are utilized to organize and control degrees of freedom of the musculoskeletal system (A. M. Williams, et al., 1999). Thus, the communication and information exchange processes within the integrated neuro-musculoskeletal system facilitate effective and efficient regulation of the involved redundant motor components and allow for coordinated movement patterns to be adapted in a dynamic performance setting (Davids, Button, Araújo, Renshaw, & Hristovski, 2006; Davids, et al., 2003; Seifert, et al., 2013).

During fundamental sport-related tasks, athletes must be able to employ different coordination patterns to address varying environmental constraints such as changes in surface properties, while still generating the desired outcome. Within these coordination patterns, functional variability in the degrees of freedom of the musculoskeletal system is necessary to adjust to changes in environmental conditions and demonstrate high movement efficacy and efficiency (Davids, Araújo, Seifert, & Orth, 2015; Davids, et al., 2006; Davids and Glazier, 2010; Hamill, et al., 2012; Newell, 1985; Rosalie and Müller, 2012).

Various non-linear methods for quantifying inter-segmental coordination variability during cyclical movements have been discussed in the literature (Glazier, Davids, & Bartlett, 2003; Komar, Seifert, & Thouvarecq, 2015; Miller, Chang, Baird, Van Emmerik, & Hamill, 2010). However since the energy-returning functions of elastic components within the musculoskeletal system during bouncing locomotion are bound by temporally-influenced properties (Wilson and Lichtwark, 2011), continuous relative phase analysis (CRP) was employed to examine coordination variability as it incorporates both spatial and temporal data. This analysis depicts segment coupling coordination during movement cycles as the difference between velocity-displacement phase angles of relative paired segments over time (Glazier, et al., 2003; Hein et al., 2012).

Continuous relative phase analyses have been utilized in a range of studies across the human movement literature. Research on athletic performance have employed CRP analyses to compare coordination variability between competition levels and task speeds in speed walking (Cazzola, Pavei, & Preatoni, 2016), over ground and treadmill running conditions (Chiu, Chang, & Chou, 2015), trained and non-trained runners (Floría, Sánchez-Sixto, Ferber, & Harrison, 2018), gender groups across different insole conditions during jump-landing tasks (Noghondar and Yazdi, 2017), phases of a 30-second vertical jump test (Pupo, Dias, Gheller, Detanico, & Santos, 2013), and countermovement jumps performed by youth and adults (Raffalt, Alkjær, & Simonsen, 2016). Studies concerned with injury have also employed CRP measures to assess whether coordination was affected by some condition including chronic ankle instability during jogging and walking (Drewes et al., 2009), low back pain during locomotion (Ebrahimi, Kamali, Razeghi, & Haghpanah, 2017; Seay, Van Emmerik, & Hamill, 2011), iliotibial band syndrome during running (Hein, et al., 2012; Miller, Meardon, Derrick, & Gillette, 2008), anterior cruciate ligament reconstruction during walking and running (Kurz, Stergiou, Buzzi, & Georgoulis, 2005), and anterior cruciate ligament deficiency during a single-step descent (Nematollahi et al., 2016). To provide the reader with sufficient evidence of the efficacy of CRP for coordination variability analysis, summaries and pertinent findings of the athletic performance (Table 2.1) and injury-related studies (Table 2.2) cited above are presented. These previous studies suggest that many factors can influence coordination and that the amount of coordination variability that demonstrated during movement is dependent on the demands and constraints of the task, environment, and organism. In light of this adaptability, the present project chose CRP as a means of determining if the differences between synthetic and natural turf systems were significant enough to yield alterations in coordination variability of lower extremity segment couplings.

Table 2.1.

Summary of cited studies pertaining athletic performance and continuous relative phase coordination variability.

Study	Aim	Participants	Task	Dependent Measures	Results	Conclusion
Cazzola, Pavei, & Preatoni, 2016	To determine whether race walking competition levels and progression speed affect coordination variability	15 male race walkers: - 4 elite - 6 international - 5 national	Race walking on a treadmill 1) 12.0 km/h 2) 15.5 km/h	Inter-segmental coordination variability - Hip-ankle sagittal coupling - Pelvis frontal- hip sagittal coupling - Pelvis transverse-hip sagittal coupling - Pelvis frontal- ankle sagittal coupling - Pelvis transverse-ankle sagittal coupling - Pelvis frontal- pelvis transverse coupling	Pelvis frontal- hip sagittal coupling coordination variability was higher for national than international and elite during early stance Pelvis transverse-ankle sagittal coupling coordination variability was higher for national than international and elite during propulsion	- Coordination variability can detect difference in competition level. - Higher competition athletes may have higher risk of more injury - More skilled mechanics may require a coordination variability to fit within a particular range.
Chiu et al., 2015	To investigate inter-joint coordination variability during over ground and treadmill walking.	5 participants: - 3 males - 2 females	<u>Walking:</u> Overground: 1) Self-selected speed (GPS) Treadmill: 1) Self-selected speed (TPS) 2) Pace that matched over-ground walking speed (TGS)	Inter-joint coordination variability during stance and swing phases: - Hip-ankle coupling - Knee–ankle coupling	<u>Stance Phase:</u> Hip-knee—No differences in coordination variability during GPS vs TPS and TGS vs TPS were observed. Coordination variability during TGS was reduced compared to GPS. Hip-ankle—No difference in coordination variability during GPS v TPS was observed. Coordination variability during TGS was reduced compared to GPS and TPS. <u>Swing Phase:</u> No differences were observed in hip-ankle or knee-ankle variability during the swing phase between any conditions. *<u>Noteworthy additional finding:</u>* *TPS walking speed was significantly less than GPS & TGS walking speeds.*	- Preferred treadmill walking speed on may be reduced to maintain similar coordination variability to that of preferred speed over ground walking.

Table 2.1. *(Continued, 2 of 3)*

Floría et al., 2018	To investigate the effect of running experience on coordination variability.	22 female participants: - 10 experienced runners (> 35km per week) - 12 unexperienced runners (< two days of recreational running per week)	Treadmill running at a self-selected, submaximal pace	Inter-joint coordination variability: - Hip-knee sagittal plane coupling - Hip-knee frontal plane coupling - Knee-ankle sagittal plane coupling	No differences were observed in inter-segment coordination variability during running between groups	- Coordination variability was not influenced by level of running experience.
Noghondar & Yazdi 2017	To investigate the influence of insole stiffness on the landing phase of a jumping task.	20 participants: - 10 male - 20 female	Jump-landing (combination of vertical and broad jump) task under three insole conditions: 1) No insole 2) Compliant insole 3) Stiff insole	Inter-segment coordination variability (standard deviations) between stepping and supporting limb: - Shank-foot coupling - Thigh-shank coupling	Shank-foot: Women demonstrated lower inter-segment coordination variability compared to men during landing with no insoles. Thigh-shank: No differences were observed in inter-segment coordination variability between groups and conditions.	Females may be able to utilize soft and stiff insole to achieve the same amount of coordination variability as men

Table 2.1. *(Continued, 3 of 3)*

Pupo, Dias, Gheller, Detanico, & Santos, 2013	To examine the modulation of intralimb coordination variability throughout a maximal continuous vertical jump test	20 male athletes: - 16 volleyball - 4 basketball	30-s continuous vertical jump test	Inter-segmental coordination variability in the sagittal plane: - Trunk-thigh coupling - Thigh-shank coupling	- Reduced trunk-thigh coupling coordination variability was observed during the concentric and eccentric phases of the initial jumps vs the final jumps - Reduced thigh-shank coupling variability was observed during the concentric phase of the initial jumps vs the final jumps	- Instability in coordination variability to greatest during take-off across both couplings during the initial and final jumps. - Fatigue appears to lead to greater inter-segmental coordination variability
Raffalt et al., 2016	To investigate the effect of age on a countermovement vertical jump task.	20 participants: - 10 Males - 10 Boys	9 maximal counter-movement vertical jumps	Inter-segmental coordination variability: - Thigh-shank coupling - Shank- foot coupling Intra-segmental coordination variability between each limb: - Thigh-thigh coupling - Shank-shank coupling - Foot-foot coupling	Inter-segmental variability: - Higher thigh-shank and shank-foot coordination variability was observed in the child group. Intra-segmental variability: - Higher thigh-thigh and shank-shank coordination variability was observed in the child group. - Foot-foot: No differences were observed coordination variability between groups	Children's coordination patterns are less consistent than adults and this ability has not yet developed through normal ontogenesis

Table 2.2.

Summary of cited studies pertaining injury and continuous relative phase coordination variability.

Article	Aim	Participants	Task	Dependent Measures	Results	Conclusion
Drewes et al., 2009	To investigate inter-segment coordination variability during walking and running tasks in the chronic ankle instable and healthy populations	14 participants: - 7 healthy - 7 chronic ankle instability	Treadmill walking at 4.83 km/h Treadmill jogging at 9.66 km/h	Inter-segmental coordination variability: - Shank–rear foot coupling (rotation-inversion/eversion)	No differences were observed in inter-segment coordination variability during the walking and jogging conditions between groups.	- Braces cause a change in neuromuscular activity during walking. - Clinicians should be aware of these changes when prescribing braces, as it may relate to the mechanism through which braces decrease sprains.
Ebrahimi, Kamali, Razeghi, & Haghpanah, 2017	To assess inter-segmental coordination variability amongst the lower extremity pelvis, and trunk, in individuals with and without nonspecific chronic low back pain (CLBP) during free-speed walking	- 10 participants with nonspecific CLBP - 10 non-CLBP controls	Free-speed walking, barefoot, 8m walkway	Inter-segmental coordination variability in the sagittal plane: - Trunk-pelvis coupling -	The CLBP group exhibited reduced trunk-pelvis and pelvis-thigh coordination variability during stance and swing compared to the non-CLBP.	- Reducing coordination variability in the trunk-pelvis and pelvis-thigh couplings may be a compensatory strategy in response to CLBP

Table 2.2. *(Continued, 2 of 3)*

Hein et al., 2012	To assess whether inter-joint coordination variability can act as a determinant of changes in running upon the onset of an injury.	18 female runners	Overground running on a 13 meter track at a velocity of 3.3 m/s.	Inter-joint coordination variability: - Hip-knee coupling - Knee-ankle coupling	No differences were observed in inter-joint coordination variability, between healthy and previously injured runners, during the running task.	- CRP variability may not be a viable method for distinguishing healthy runners from injured runners, participant when dealing with small sample sizes.
Miller et al., 2008	To assess whether inter-joint coordination variability can act as a determinant of changes in running upon the onset of iliotibial band syndrome.	16 recreational runners: - 8 healthy participants - 8 participants with a history of iliotibial band syndrome	Treadmill running at a self-selected pace for 20 minutes.	Inter-segmental coordination variability throughout the beginning, middle, and end of the running task: - Thigh-shank coupling - Thigh-foot coupling - Shank-foot coupling - Knee-foot coupling	Thigh-shank: No differences were observed in inter-segment coordination variability, between healthy and previously injured runners, during the running task. Thigh-foot: Lower inter-segment variability was observed in the iliotibial band syndrome group at the end of a running task. Shank-foot: No differences were observed in inter-segment coordination variability, between healthy and previously injured runners, during the running task. Knee-foot: Lower inter-segment variability was observed in the healthy group at the beginning of a running task.	- History of ITBS may be linked to altered coordination variability amongst injury-related segment couplings

Table 2.2. *(Continued, 3 of 3)*

Nematollahi et al., 2016	To investigate inter-segment coordination variability during a stepping task between healthy and anterior cruciate ligament (ACL) deficient populations.	46 participants: - 23 healthy participants - 23 ACL deficient participants	Stepping down from a 21 cm high step	Inter-segmental coordination variability within the stepping and supporting limbs: - Shank-foot coupling - Thigh-shank coupling	<u>Supporting Limb</u>: Shank-foot: The healthy group demonstrated higher coordination variability at initial contact Thigh-shank: The anterior cruciate ligament deficient group demonstrated higher coordination variability at initial contact. <u>Stepping Limb:</u> Shank-foot: The anterior cruciate ligament deficient group demonstrated higher coordination variability at initial contact. Thigh-shank: The anterior cruciate ligament deficient group demonstrated higher coordination variability at initial contact.	- Individuals with deficient ACLs may present altered coordination strategies including increased variability.
Seay et al., 2011	To investigate the influence of variations in low back pain on running	42 participants: - 14 healthy - 14 lower back pain - 14 resolved lower back pain	Walk to run transition at 30 s increments: started at .8 m/s and progressed to 3.8 m/s (with .5 m/s increments)	Inter-segmental coordination variability: - Trunk-pelvis coupling	Decreased coordination variability in the lower-back pain group compared to the healthy group.	- Even one bout of low back pain may be linked to increased risk of injury and detriments to performance

Synthetic and Natural Turf

The suitability of synthetic turf systems for serving as an alternative athletic playing surface to natural grass is a discussion that continues to receive attention on both a national and international scale. Due to continued innovations in the sports turf industry, athletes are being tasked with playing on varying types of synthetic turf systems as well as natural turf fields. By adjusting or even changing the components of synthetic turf systems, such as the pile height, type of the carpet fibers, the shock pad, and the infill makeup, manufacturers have improved athlete-related properties of the surface, such as vertical deformation and energy return (Fleming, 2011). These synthetic turf properties are intended to mimic performance and safety characteristics of natural grass (the gold standard) as closely as possible, but they still differ to a degree (Fleming, 2011; Severn, et al., 2008).

Research on athlete perceptions, performance, and injuries in relation to synthetic versus natural turf surfaces offer conflicting evidence both for and against synthetic turf. Interestingly, qualitative reports from athletes indicate that athletes perceive there to be differences between synthetic and natural turf (Andersson, Ekblom, & Krustrup, 2008) even though both surfaces have been tested to meet the performance and safety standards of the governing agencies for the intended sport (Charalambous, und Wilkau, Potthast, & Irwin, 2016; Meijer, Dethmers, Savelberg, Willems, & Wijers, 2007). Furthermore, while some evidence suggests that performance on synthetic turf is not different than performance on natural turf, others contend that synthetic turf superior (Choi, Sum, & Leung, 2015; Gains, Swedenhjelm, Mayhew, Bird, & Houser, 2010). A similar trend can be seen in research analyzing injury reports where the findings are largely inconsistent especially between different sports, generating cause for skepticism regarding the validity of their findings (Dragoo and Braun, 2010; Ekstrand, Hägglund, & Fuller, 2011; Ekstrand, Timpka, & Hägglund, 2006; Fuller, Dick, Corlette, & Schmalz, 2007a, 2007b; Meyers, 2013, 2017; S. Williams, Hume, & Kara, 2011).

Auspiciously, a recent study by Mack et al. (2018) addressed inconsistencies in the literature specifically regarding injuries on synthetic versus natural turf surfaces. The authors brought to light some of the flaws of previous studies and emphasized the importance of taking a biomechanical approach to analyzing reported injury data. They asserted that their hypotheses were formed based on shoe-surface interaction studies that have shown that synthetic turf does not release the cleat from the surface as quickly as natural turf during rotation. By using these hypotheses to account for grades of injury, anatomic locations, and mechanisms (i.e., contact versus non-contact) of injuries, as well as the type of field on which the injury occurred, their analysis revealed a causal link between turf type and injuries. This signifies the value and necessity of biomechanics research in understanding the influence of synthetic and natural turf on athlete performance and safety.

Summary

As the number of synthetic turf fields continues to grow, the need for understanding how these surfaces influence injury and performance also grows. While developments in synthetic turf have helped to reduce dissimilarities between synthetic turf and natural turf, differences in key physical properties such as surface stiffness still exist (Fleming, 2011; Severn, et al., 2008). By investigating vertical and leg stiffness as well as coordination variability on different synthetic turf surfaces and natural turf, much needed insight on how the body interprets and responds to the stiffness of these surfaces can be gained. This information is valuable for athletes preparing to compete on these surfaces as well as turf manufacturers concerned with athlete performance and safety.

CHAPTER 3

Methods

This section presents an inclusive summary of all methodology employed in this project.

Participants

An a priori power analysis was conducted to determine the sample size needed for this study (G*Power, Version 3.1.9.2). The parameters for the analysis were set as follows: power of 0.80, a type I error rate threshold of 0.05, a medium effect size of 0.25, a correlation coefficient between repeated measures of 0.70, and a nonsphericity correction of 1 to determine a sample size of 15. Seventeen participants (age: 23.1 ± 2.9 years; height: 1.81 ± 0.06 m; mass: 77.8 ± 9.9 kg) were recruited from the surrounding community for the study. All participants indicated their voluntary involvement by signing an informed consent approved by the Institutional Review Board prior to participation. Participants completed a health-history questionnaire to determine eligibility in this study. Inclusion criteria included males in good self-reported health, minimum high school athletic experience of two years, and participation in a minimum of three days of moderate to vigorous physical activity a week. Exclusion criteria included current or recent lower extremity injury within the last three months, prior injury to the lower extremity that required surgery, and allergy to adhesive.

Table 3.1.

Turf System Specifications of Each Testing Surface

	Fiber Type	Pile Height (in)	Shock Pad (mm)	Infill Composition	Face Weight (oz/yd^2)	Firmness (mm)
Synthetic Turf 1	Dual Fiber Hybrid (slit-film fiber and monofilament fiber)	2.25 in	None	60% sand, 40% rubber	46	5.65
Synthetic Turf 2	Dual Fiber Hybrid (slit-film fiber and monofilament fiber)	2.0 in	14 mm	60% sand, 40% rubber	46	6.66
Synthetic Turf 3	Dual Fiber Hybrid (slit-film fiber and monofilament fiber)	1.75 in	14 mm	90% coconut husk/fibers, 10% naturally derived plant-based matter	46	6.89
	Grass Type	Height of Cut (in)		Soil Composition		
Natural Turf	Tifway Bermudagrass	5/8 in		Loamy sand, 2.1% organic matter		7.04

Note. Firmness represents surface deformation.

Design and Protocol

In order to determine the influence of different turf surfaces on select biomechanical movement variables, we chose to test four different turf surfaces—three synthetic turf surfaces and one natural turf (Table 3.1). To reduce the risk of fatigue, data collection was split into two sessions held on separate days with two of the four surfaces tested per session. The surface testing order was determined per participant by random selection of a starting point within the following cyclic order of test surfaces: synthetic turf 1, synthetic turf 2, synthetic turf 3, and natural turf.

Since data collection took place at an outdoor turf field laboratory, there were certain conditions that could not be controlled for, but actions were taken to reduce their influence on the testing environment. Surface and ambient temperatures were not controlled for, but both days of data collection for every participant took place at the same general time of day (i.e., either in early morning, late morning, midday, early afternoon, or late afternoon). Additionally, surface moisture content was not controlled. However, to avoid the influence of excessive moisture, data collections did not take place after rainfall until a full day had passed.

Upon arriving at the outdoor turf field laboratory, participant's height, mass, and foot length measurements were recorded, and they were fitted with a new pair of cleats to be worn during the study. Substantial evidence has demonstrated the complexity of the cleat-ground interface and revealed that various elements of cleat design, such as stud configuration and shape, upper, heel cup, and shoe plate stiffness are known to influence the shoe-ground interaction (Clarke and Carré, 2010; Hennig and Sterzing, 2010; Kulessa, Gollhofer, & Gehring, 2017; C. Müller, Sterzing, Lake, & Milani, 2010; C. Müller, Sterzing, Lange, & Milani, 2010; Schrier, Wannop, Lewinson, Worobets, & Stefanyshyn, 2014; Severn, et al., 2008; Silva et al., 2017). Thus to minimize potential variations induced by differences in cleat models across participants, each individual wore one of two provided models (Figure 3.1). Both models had the same upper, heel, and shoe plate construction including stud configuration and differed in mass by less than 1 g.

Figure 3.1. Cleat models used in this study. (A) Under Armour Speedform® MC, (B) Under Armour Spotlight.

Eight wireless inertial measurement unit (IMU) sensors (MTw, Xsens Technologies B.V., Enschede, the Netherlands) were affixed bilaterally to the feet, lower legs, and thighs as well as to the pelvis and trunk (Figure 3.2). To ensure the sensors were firmly affixed yet not restricting movement, the foot trackers were secured to the top of the cleats with athletic tape and the remaining sensors were attached directly to the skin with elastic adhesive bandage (Cover-Roll™; BSN Medical, Beiersdorf AG, Hamburg, Germany). Shank and thigh sensors were further secured with foam prewrap (Z – wrap, Johnson & Johnson, Langhorne, PA, USA). Sensor-to-segment calibration was then carried out by having the participant assume a static neutral pose, walk forward approximately 3 meters from the location of the static pose, and then walk back to the same location and resume a static neutral pose (Xsens, MVN MTw User Manual, 2018).

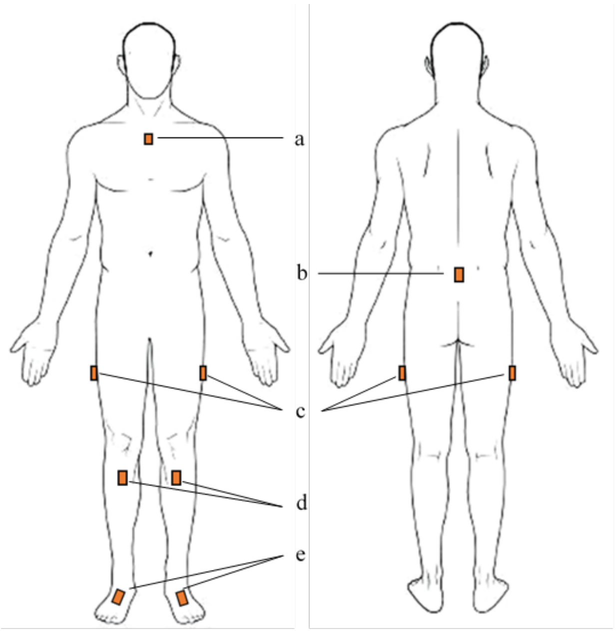

Figure 3.2. IMU sensor placement based on Xsens MVN MTw User Manual (2018). (a) Trunk Sensor – sternum just below the sternal angle, (b) Pelvis Sensor– sacral bone between left and right iliac spine, (c) Thigh Sensors – lateral thigh midway between greater trochanter and lateral femoral epicondyle, (d) Shank Sensors – flat surface medial to the tibial tuberosity, (e) Foot Sensors – Dorsal surface just distal to the navicular.

Prior to testing, each participant was allotted unlimited time to perform their typical individual warm-up routine. For both data collection days, warm-up routines lasted 10 minutes on average and included light jogging, static and dynamic lower extremity stretches, and short distance runs. On each of the four turf surfaces, participants performed three trials of a single leg hopping task and a submaximal 35-m running task. The task order was randomized for each participants and each surface. For the single leg hopping trials, participants were instructed to hop in place ten times at a steady, self-selected frequency, on their dominant limb with their hands resting on their hips. Leg dominance was defined as the leg identified by each participant as his preferred kicking leg (Granata, Padua, & Wilson, 2002; Hobara et al., 2010; Mudie, Gupta, Green, Hobara, & Clothier, 2017; Padua et al., 2006). For the submaximal 35-m running trials, the participants were instructed to run the set distance at a steady, submaximal, self-selected frequency. Since constraining movement frequencies to a target pace is known to influence movement parameters (Auyang, Yen, & Chang, 2009; Hobara, et al., 2010), self-selected frequencies for both tasks were chosen in order to measure the participant's authentic, unaltered response to each surface.

Data Acquisition and Processing

Synchronized three-dimensional accelerometer and gyroscope signals internally sampled at >1000 Hz and magnetometer signals sampled at >100Hz by each IMU sensor were transferred wirelessly amongst each other as well as to the Awinda base station connected to the data collection workstation. Using the Xsens MVN Analyze software engine (Version 2019.0, Enschede, the Netherlands), the sampled signals from each sensor were processed frame-by-frame using advanced sensor fusion algorithms and advanced biomechanical models, resulting in stable motion tracking at a rate of 100 Hz. After each trial, data were reprocessed over a larger window of frames with the Reprocess HD function to obtain optimal estimates of six-degree-of-freedom kinematics for each segment (Schepers, Giuberti, & Bellusci, 2018).

Linear and angular kinematic data for all surfaces were exported from MVN Analyze at 100 frames per second and imported into Visual3D software (C-Motion, Germantown, Maryland, USA) for additional processing. Center of mass height at each time (COMz) was estimated instantaneously at each time point (t) using segment center of mass vertical positions and masses of the feet, shanks, thighs, pelvis, and trunk. Segment masses and vertical center of mass locations were calculated as proportions of the total body mass and the participant's height (Dempster, 1955; Hanavan Jr, 1964). To account for the mass of the head and arms for which kinematic data were not collected, the segment parameters of the trunk were adjusted to represent the trunk, arms, and head as a rigid unit. The equation used is as follows:

$$COMz(t) = \frac{1}{M}\sum_{i=1}^{N} m_i z_i\,(t) \qquad (1)$$

where M was the total body mass, N was the total number of segments, m_i was the mass of a segment, z_i was the vertical position of the segment center of mass at time point t (Mudie, et al., 2017; Ranavolo et al., 2008; Saini, Kerrigan, Thirunarayan, & Duff-Raffaele, 1998).

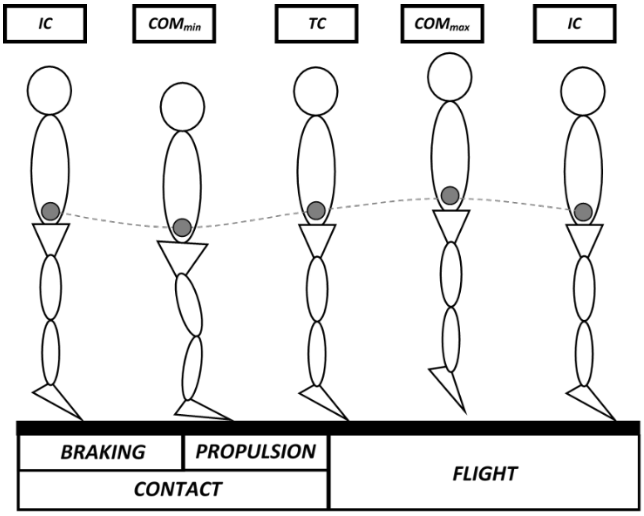

Figure 3.3. Phases, sub-phases, and key events of hopping. IC = initial contact, COM_{min} = center of mass minimum height, TC = terminal contact, COM_{max} = center of max maximum height.

Hopping (Figure 3.3) and running (Figure 3.4) cycles were defined as the time series between the instant of terminal ground contact (i.e., toe off) to the subsequent instance of terminal ground contact for the same foot (Cavagna, Franzetti, Heglund, & Willems, 1988; Gutmann and Bertram, 2017; Novacheck, 1998; Serpell, et al., 2012). These cycles were then broken down into two phases—flight phase (or aerial phase) and contact phase (or stance phase). The flight phase of hopping was defined from terminal ground contact to subsequent initial ground contact (Blickhan, 1989; Waxman, Ford, Nguyen, & Taylor, 2018). The flight phase of running was defined from terminal ground contact of the non-dominant foot to the subsequent initial ground contact of the dominant foot (Blickhan, 1989; Novacheck, 1998; Padulo, Chamari, & Ardigò, 2014). For hopping and running cycles, contact phase was defined from initial ground contact of the dominant foot to terminal ground contact of the same foot.

The contact phases of running and hopping were dived into two sub-phases of interest—braking and propulsion. Typically, the instant of peak vertical ground reaction force marks the transition from braking to propulsion (Caderby and Dalleau, 2018; Cavagna, Saibene, & Margaria, 1964; Kuitunen, Ogiso, & Komi, 2011; Ranavolo, et al., 2008), and whole body center of mass minimum height (COM_{max}) is also observed at this time point in the contact phase (Brughelli and Cronin, 2008; Buchheit, et al., 2015; Caderby and Dalleau, 2018; Ferris and Farley, 1997) (Figure 3.5). Thus since ground reaction forces were not directly measured in this study, the braking sub-phase was alternatively defined from initial ground contact to the instant of maximum center of mass vertical displacement, and the propulsion sub-phase defined from instant of maximum center of mass vertical displacement to terminal ground contact. Initial contact and terminal ground contact events were created with user-defined peak detection pipeline commands that automatically identified distinctive local maxima in the resultant linear

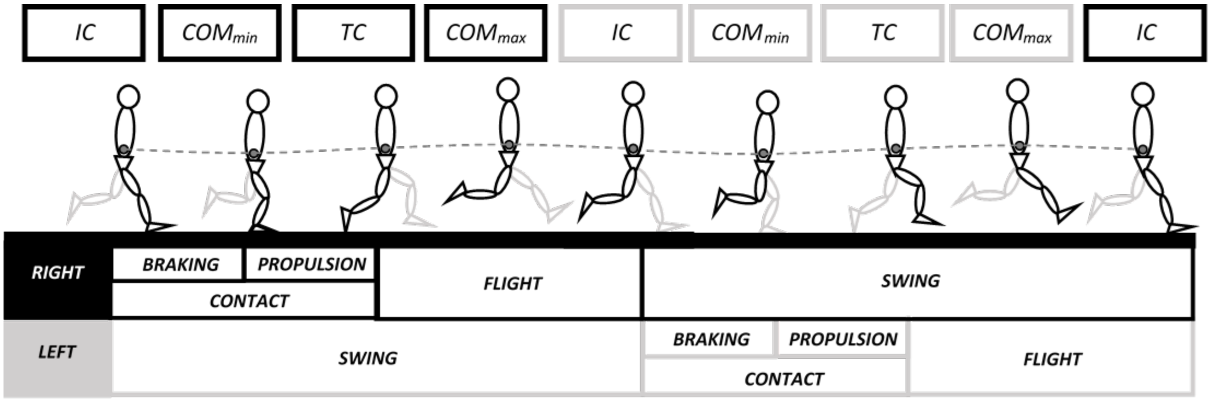

Figure 3.4. Phases, sub-phases, and events of running. IC = initial contact, COM_{min} = center of mass minimum height, TC = terminal contact, COM_{max} = center of max maximum height.

acceleration and angular velocity magnitudes of the foot, respectively (Bergamini et al., 2012; Reenalda, Maartens, Buurke, & Gruber, 2019; Reenalda, Maartens, Homan, & Buurke, 2016; Sabatini, Martelloni, Scapellato, & Cavallo, 2005; Strohrmann, Harms, Kappeler-Setz, & Troster, 2012).

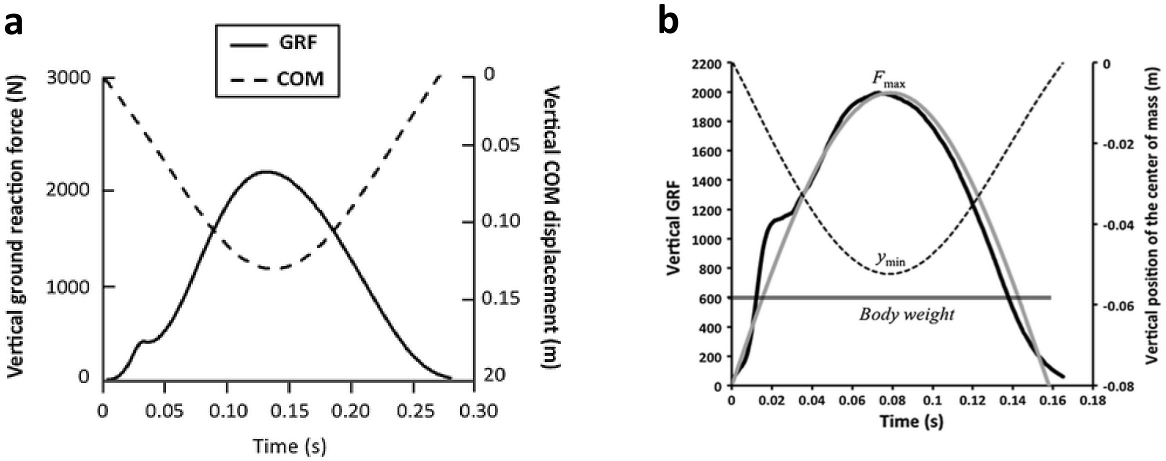

Figure 3.5. Concurrent timing of peak vertical ground reaction force and maximum vertical center of mass displacement during: (a) hopping [Adapted from Caderby and Dalleau (2018)] and (b) running [Adapted from Morin (2018)].

Events delineating the phase of hopping and running phases were created with a pipeline of user-defined peak detection algorithm commands. Local minima in the vertical center of mass position time series were identified as minimum center of mass height (COM_{min}). For the purpose of narrowing the window scanned for ground contact events, local maxima directly proceeding each COM_{min} were identified as maximum center of mass height (COM_{max}). Terminal ground contact events were identified between COM_{min} and COM_{max} as local maxima in the sagittal plane angular velocity time series of the foot. Initial ground contact events were identified between COM_{max} and COM_{min} at local maxima in the resultant linear acceleration time series of the foot (Bergamini, et al., 2012; Reenalda, et al., 2019; Reenalda, et al., 2016; Sabatini, et al., 2005; Strohrmann, et al., 2012). Following event creation, trials were inspected in order to detect any erroneous data or missing events within the hopping or running cycles.

Stiffness Measures.

Stiffness measures during hopping and running were computed using the middle three cycles of each trial to eliminate misrepresentative variability caused by movement initiation and termination. For both tasks, vertical stiffness (K_{vert}) was computed as the ratio of peak vertical ground reaction force ($peak\ GRF_{vert}$) to center of mass vertical displacement (ΔCoM_{vert}). Leg stiffness (K_{leg}), was also computed during the hopping and running trials. Leg stiffness computation differs from the vertical stiffness computation is only in the denominator, where instead of using ΔCoM_{vert}, the change in leg length (ΔL_{leg}) from standing length to the maximum shortened length during stance phase was used. The actual maximum shortened leg length during the running trials is typically measured as the distance from the center of pressure location along the foot to the greater trochanter or hip. However since center of pressure data was not measured in this study, the resultant distance from the position of the proximal end of the thigh (representative of the greater trochanter) to distal end of the shank (representative of the lateral malleoli) was used as a surrogate measure during both standing and during the running trials (DuBose et al., 2017). The locations of segment ends were modeled based on segment lengths calculated as a proportion of total height and the linear positions and relative rotations of the foot, shank, and thigh segments (Drillis, Contini, & Bluestein, 1969; Schepers, et al., 2018; Winter, 2009).

To estimate peak vertical ground reaction force ($peak\ GRF_{vert}$), the sine wave method previously validated for both hopping and running for field-based measures (Dalleau, Belli, Viale, Lacour, & Bourdin, 2004; Morin, Dalleau, Kyröläinen, Jeannin, & Belli, 2005) was employed (Appendix A). In this method, *peak* GRF_{vert} is modeled using following equation:

$$peak\ GRF_{vert} = m \cdot g \cdot \frac{\pi}{2} \cdot \left(\frac{T_f}{T_c} + 1\right) \tag{2}$$

where m is the body mass in kg, g is gravitational acceleration, T_f is flight time, T_c is contact time. Contact and flight times were defined from initial ground contact to terminal ground contact and terminal ground contact to initial ground contact, respectively.

Using the vertical position of the center of mass estimated using Equation 1, center of mass vertical displacement (ΔCoM_{vert}) was calculated as:

$$\Delta CoM_{vert} = CoM_{vert\_@initial\ ground\ contact} - COM_{vert_{@minimum\ height}} \tag{3}$$

Vertical stiffness (K_{vert}) was then measured during hopping and running using Equation 2 in the numerator and Equation 3 in the denominator:

$$K_{vert} = \frac{peak\ GRF_{vert}}{\Delta CoM_{vert}} \tag{4}$$

During running only, leg stiffness (K_{leg}) was computed as:

$$K_{leg} = \frac{peak\ GRF_{vert}}{\Delta L_{leg}} \tag{5}$$

using Equation 2 in the numerator and the following equation for ΔL_{leg} in the denominator:

$$\Delta L_{leg} = L_{standing} - L_{maximum\ compression} \tag{6}$$

The vertical and leg stiffness values were originally computed in units of N/m but were normalized by body weight (BW) and leg length (L) to account for anthropometric variations between participants. Thus, the stiffness values reported are unitless but should be interpreted units of BW/L.

In addition to vertical and leg stiffness, self-selected hopping and stride frequencies were computed. Hop frequency was calculated as the reciprocal of the duration of the hopping cycle (Farley, et al., 1991; Kuitunen, et al., 2011; Mudie, et al., 2017; Ranavolo, et al., 2008). Similarly, stride frequency was computed as the reciprocal of the duration of the running cycle (Cavagna, et al., 1964; Farley and Gonzalez, 1996; Padulo, et al., 2014).

Coordination Variability Measures.

Absolute segment angular displacements were computed relative to the right horizontal of global sagittal and frontal planes (Figure 3.6). Afterward, absolute segment angular velocities were computed as the first derivative of the segment angular displacements. To ensure steady movement, time series data for these parameters were sampled during the braking and propulsion sub-phases for only the fourth, fifth, and sixth hopping and running cycles of each trial.

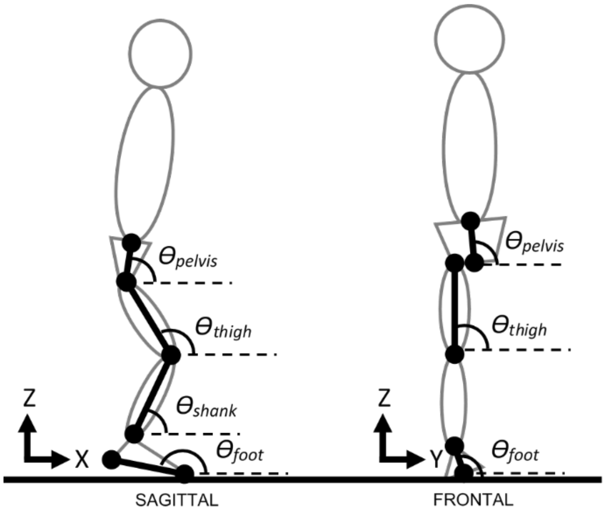

Figure 3.6. Absolute segment angles computed relative to the global sagittal and frontal planes.

Braking and propulsion data samples were then extrapolated to 101 data points to enable mean ensemble data to be calculated at 1% intervals (Smallmana, Graham, & Stevenson, 2013).

Extrapolated segment angular displacement and angular velocity data from each braking and propulsion sample of each trial were exported to MATLAB® for additional processing (R2016a, Mathworks, Inc., Natick, MA). Using custom code, the following procedures were executed for the hopping and running braking and propulsion sub-phases separately and for each turf to compute CRP variability for the following segment couplings of interest: pelvis-thigh, thigh-shank, thigh-foot, and shank-foot sagittal plane couplings and pelvis-thigh and thigh-foot frontal plane couplings. Two normalization procedures were employed to account for individual frequency and amplitude variations. These procedures also ensure that a normalized angular displacement value of zero represents the midpoint of the dynamic range of motion and an angular velocity value zero continues to represent no change in angular displacement occurring at that time point (Hamill, et al., 1999; Lamb and Stöckl, 2014; Miller, et al., 2010; Miller, et al., 2008; Peters, Haddad, Heiderscheit, Van Emmerik, & Hamill, 2003; Prejean and Ricard, 2019). Angular displacements (θ) were normalized per trial by setting the minimum angle at −1, the maximum angle as 1, and midpoint at 0:

$$\theta_{i,norm} = \frac{2*[\theta_i - \min(\theta)]}{\max(\theta) - \min(\theta)} - 1 \qquad (2)$$

where *i* represents each of the 101 data points in the time series (Hamill, et al., 1999). Angular velocities (ω) were normalized per trial by setting the absolute maximum angular velocity of the time series as ±1:

$$\omega_{i,norm} = \frac{\omega_i}{\max(|\omega|)} \qquad (3)$$

Using the normalized angular displacement and velocity data for each segment, phase angles (φ) were calculated between -180° and 180° at each point in the time:

$$\varphi_i = \tan^{-1}\left(\frac{\omega_{i,norm}}{\theta_{i,norm}}\right) \tag{4}$$

From these phase angles, relative phase angles (Φ) for each of the segment couplings of interest were computed at each point of the time series by subtracting the phase angle of the distal segment from the phase angle of the proximal segment:

$$\Phi = \varphi_{proximal} - \varphi_{distal} \tag{5}$$

The relative phase angles at each point of the time series were averaged across all samples from all trials (*N* = 9 per participant) to generate mean ensemble CRP angles and standard deviations. The standard deviations of the ensemble CRP angles across all 101 data points were averaged to quantify CRP variability:

$$CRPvariability = \frac{\sum_{i=1}^{N} SD_i}{N} \tag{6}$$

The outcome of these computations is a single CRP variability value that is representative of the average amount of coordination variability observed.

Statistical Analysis

Data were analyzed using statistical software (SPSS, Version 25.0, SPSS Inc, Chicago, IL, USA). The distribution of the data was assessed with Shapiro-Wilk tests and failed to meet the assumption of normality. Therefore, nonparametric analyses were performed to assess for differences in stiffness, frequency, and CRP variability among the four turf surfaces. Repeated measures Friedman ANOVA by ranks tests were conducted for each parameter measured Statistical significance was set a priori at α = .05.

CHAPTER 4

Investigation of leg spring behavior during hopping and running on natural and synthetic turf playing surfaces

Keywords: Synthetic turf, natural turf, vertical stiffness, leg stiffness, biomechanics

Introduction

The mechanical behavior of the body during bouncing locomotion is modeled as a simple linear mass-spring system. In this model, the body's center of mass serves as a point mass that is supported by a massless spring (Blickhan, 1989; Farley, et al., 1991; Farley, et al., 1985; Farley and Gonzalez, 1996; McMahon and Cheng, 1990). The lower extremity is said to act in a spring-like manner when it resists compression during loading and is described by a characteristic known as stiffness (Brughelli and Cronin, 2008; Farley, et al., 1985; Kerdok, et al., 2002; Serpell, et al., 2012). Stiffness is regulated through contributions of ligaments, tendons, bones, and muscles and plays an important role in controlling center of mass movement during hopping and running (Farley and Ferris, 1998; Maquirriain, 2013; Millett, Moresi, Watsford, Taylor, & Greene, 2018).

Investigations of stiffness during submaximal locomotion on stiff and compliant surfaces have observed adaptive capabilities of the leg spring (Farley, et al., 1998; Ferris and Farley, 1997; Ferris, et al., 1999; Ferris, et al., 1998; Karamanidis, et al., 2006; Kerdok, et al., 2002). Specifically, these studies have indicated that leg stiffness, defined as resistance to change in leg length, can be adjusted during hopping and submaximal running to counter the stiffness of the surface. Thus, the effective vertical stiffness, defined in this context as the combined series stiffness of the body and the surface, remains consistent across different surfaces (Farley, et al., 1998; Ferris and Farley, 1997; Ferris, et al., 1998). Similar leg stiffness alteration strategies have been seen on even very compliant surfaces that experience noticeable deformation (i.e., foam) and on uneven surfaces (Ferris, et al., 1999; Grimmer, et al., 2008; Karamanidis, et al., 2006; Kerdok, et al., 2002). These findings suggest that the body will exploit the adjustable stiffness properties of the lower extremity to respond to various environmental demands.

During hopping and running, two prevalent movements in sports, keeping vertical stiffness consistent across different surfaces is considered to be an essential locomotive control strategy for conserving center of mass dynamics and has been suggested to be important for optimizing movement efficiency (Kerdok, et al., 2002; Moritz and Farley, 2004). Athletes who appropriately adapt leg stiffness and maintain vertical stiffness during these motion may potentially reduce the onset of fatigue and improve performance through storage of elastic energy during landing or braking and returning energy during propulsion (Brazier, et al., 2014; Butler, et al., 2003). Additionally, effective reductions in leg stiffness are important in situations where impact attenuation is necessary to protect the system from excessive forces during loading (Brazier, et al., 2014). Conversely, it is important to note that a lack of appropriate adaptation in stiffness can be detrimental. Excessive lower limb stiffness is believed to increase injury risk to bone tissue due to repetitive loads transmitted through minimally flexed lower extremity joints (Butler, et al., 2003; Williams III, et al., 2004; Williams III, et al., 2001). In addition, a lack of stiffness in the leg spring has implications for elevated risk of soft tissue damage (e.g., muscle strain) as a result of increased muscular demand needed for force attenuation (Butler, et al., 2003; Pickering Rodriguez, et al., 2017; Williams III, et al., 2004; Williams III, et al., 2001)

The ability to adapt lower extremity stiffness is useful for meeting a range movement goals in a dynamic environment, especially for athletes tasked with playing on different surfaces like synthetic and natural turf. As the number of synthetic turf fields continues to grow, the need for understanding how these surfaces influence injury and performance also grows. While developments in synthetic turf have helped to reduce dissimilarities between synthetic turf and natural turf, differences in key physical properties such as surface stiffness still exist (Fleming, 2011; Severn, et al., 2008). By investigating vertical and leg stiffness on different synthetic turf surfaces and natural turf, much needed insight on how the body interprets and responds to the stiffness of these surfaces will be gained. This information is valuable for athletes preparing to compete on these surfaces as well as turf manufacturers concerned with athlete performance and safety.

The purpose of this study was to determine whether leg and vertical stiffness during hopping and running are influenced by four different turf surfaces—three synthetic turf surfaces and one natural turf surface. We hypothesized that leg stiffness would be greatest on natural turf and progressively less on synthetic turf 3, synthetic turf 2, and synthetic turf 1, respectively. We also hypothesized that vertical stiffness would not differ between any of the turf surfaces. Since research has demonstrated that changes in hopping and stride frequency can serve as an alternative adaptive strategy to modulate stiffness (Cavagna, et al., 1988; Farley, et al., 1991; Farley and Gonzalez, 1996), the self-selected frequencies observed on each turf were also examined.

Methods

Participants.

An a priori power analysis was conducted to determine the sample size needed for this study (G*Power, Version 3.1.9.2). The parameters for the analysis were set as follows: power of 0.80, a type I error rate threshold of 0.05, a medium effect size of 0.25, a correlation coefficient between repeated measures of 0.70, and a nonsphericity correction of 1 to determine a sample size of 15. Seventeen participants (age: 23.1 ± 2.9 years; height: 1.81 ± 0. 06 m; mass: 77.8 ± 9.9 kg) were recruited from the surrounding community for the study. All participants indicated their voluntary involvement by signing an informed consent approved by the Institutional Review Board prior to participation. Participants completed a health-history questionnaire to determine eligibility in this study. Inclusion criteria included males in good self-reported health, minimum high school athletic experience of two years, and participation in a minimum of three days of moderate to vigorous physical activity a week. Exclusion criteria included current or recent lower extremity injury within the last three months, prior injury to the lower extremity that required surgery, and allergy to adhesive.

Design and Protocol.

In order to determine the influence of different turf surfaces on select biomechanical movement variables, we chose to test four different turf surfaces—three synthetic turf surfaces and one natural turf surface (Table 4.1). To reduce the risk of fatigue, data collection was split into two sessions held on separate days with two of the four surfaces tested per session. The surface testing order was determined per participant by random selection of a starting point within the following cyclic order of test surfaces: synthetic turf 1, synthetic turf 2, synthetic turf 3, and natural turf.

Table 4.2.

Turf System Specifications of Each Testing Surface

	Fiber Type	Pile Height (in)	Shock Pad (mm)	Infill Composition	Face Weight (oz/yd$^{2)}$	Firmness (mm)
Synthetic Turf 1	Dual Fiber Hybrid (slit-film fiber and monofilament fiber)	2. 25 in	None	60% sand, 40% rubber	46	5. 65
Synthetic Turf 2	Dual Fiber Hybrid (slit-film fiber and monofilament fiber)	2. 0 in	14 mm	60% sand, 40% rubber	46	6. 66
Synthetic Turf 3	Dual Fiber Hybrid (slit-film fiber and monofilament fiber)	1. 75 in	14 mm	90% coconut husk/fibers, 10% naturally derived plant-based matter	46	6. 89
	Grass Type	Height of Cut (in)		Soil Composition		
Natural Turf	Tifway Bermudagrass	5/8 in		Loamy sand, 2. 1% organic matter		7. 04

Note. Firmness represents surface deformation.

Since data collection took place at an outdoor turf field laboratory, there were certain conditions that could not be controlled for, but actions were taken to reduce their influence on the testing environment. Surface and ambient temperatures were not controlled for, but both days of data collection for every participant took place at the same general time of day (i.e., either in early morning, late morning, midday, early afternoon, or late afternoon). Additionally, surface moisture content was not controlled. However, to avoid the influence of excessive moisture, data collections did not take place after rainfall until a full day had passed.

Upon arriving at the outdoor turf field laboratory, participant's height, mass, and foot length measurements were recorded, and they were fitted with a new pair of cleats to be worn during the study. Substantial evidence has demonstrated the complexity of the cleat-ground interface and revealed that various elements of cleat design, such as stud configuration and shape, upper, heel cup, and shoe plate stiffness are known to influence the shoe-ground interaction (Clarke and Carré, 2010; Hennig and Sterzing, 2010; Kulessa, et al., 2017; C. Müller, T. Sterzing, M. Lake, et al., 2010; C. Müller, T. Sterzing, J. Lange, et al., 2010; Schrier, et al., 2014; Severn, et al., 2008; Silva, et al., 2017). Thus, to minimize potential variations induced by differences in cleat models across participants, each individual wore one of two provided models (Figure 4.1). Both models had the same upper, heel, and shoe plate construction including stud configuration, and cleats of the same size differed in mass between models by less than 1 g.

Figure 4.1. Cleat models used in this study. (A) Under Armour Speedform® MC, (B) Under Armour Spotlight.

Eight wireless inertial measurement unit (IMU) sensors (MTw, Xsens Technologies B.V., Enschede, the Netherlands) were affixed bilaterally to the feet, lower legs, and thighs as well as to the pelvis and trunk (Figure 4.2). To ensure the sensors were firmly affixed yet not restricting movement, the foot trackers were secured to the top of the cleats with athletic tape and the remaining sensors were attached directly to the skin with elastic adhesive bandage (Cover-Roll™; BSN Medical, Beiersdorf AG, Hamburg, Germany). Shank and thigh sensors were further secured with foam prewrap (Z – wrap, Johnson & Johnson, Langhorne, PA, USA). Sensor-to-segment calibration was then carried out by having the participant assume a static neutral pose, walk forward approximately 3 meters from the location of the static pose, and then walk back to the same location and resume a static neutral pose (Xsens, MVN MTw User Manual, 2018).

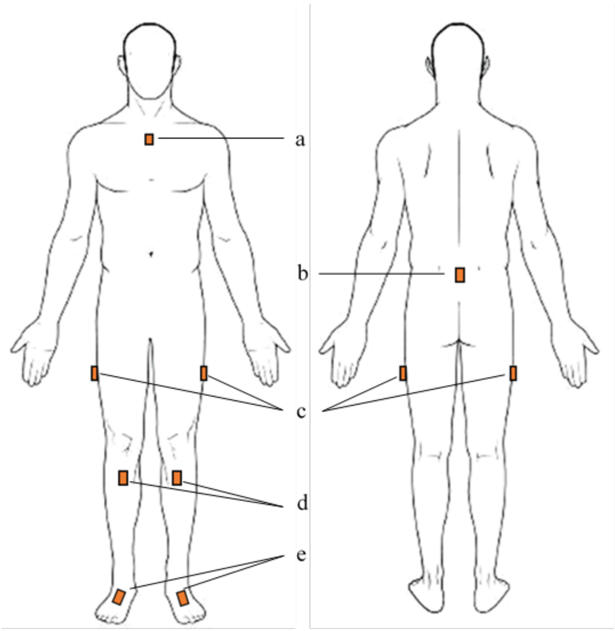

Figure 4.2. IMU sensor placement based on Xsens MVN MTw User Manual (2018). (a) Trunk Sensor – sternum just below the sternal angle, (b) Pelvis Sensor– sacral bone between left and right iliac spine, (c) Thigh Sensors – lateral thigh midway between greater trochanter and lateral femoral epicondyle, (d) Shank Sensors – flat surface medial to the tibial tuberosity, (e) Foot Sensors – Dorsal surface just distal to the navicular.

Prior to testing, each participant was allotted unlimited time to perform their typical individual warm-up routine. For both data collection days, warm-up routines lasted 10 minutes on average and included light jogging, static and dynamic lower extremity stretches, and short distance runs. On each of the four turf surfaces, participants performed three trials of a single leg hopping task and a submaximal 35-m running task. The task order was randomized for each participants and each surface. For the single leg hopping trials, participants were instructed to hop in place ten times at a steady, self-selected frequency, on their dominant limb with their hands resting on their hips. Leg dominance was defined as the leg identified by each participant as his preferred kicking leg (Granata, et al., 2002; Hobara, et al., 2010; Mudie, et al., 2017; Padua, et al., 2006). For the 35-m submaximal running trials, the participants were instructed to run the set distance at a steady, submaximal, self-selected frequency. Since constraining movement frequencies to a target pace is known to influence movement parameters (Auyang, Yen, & Chang, 2009; Hobara et al., 2010), self-selected frequencies for both tasks were chosen in order to measure the participant's authentic, unaltered response to each surface.

Data Acquisition and Processing.

Synchronized three-dimensional accelerometer, gyroscope, and magnetometer signals internally sampled at >1000 Hz by each IMU sensor were transferred wirelessly amongst each other as well as to the Awinda base station connected to the data collection workstation. Using the Xsens MVN Analyze software engine (Version 2019.0, Enschede, the Netherlands), the sampled signals from each sensor were processed frame-by-frame using advanced sensor fusion algorithms and advanced biomechanical models, resulting in stable motion tracking at a rate of 100 Hz. After each trial, data were reprocessed over a larger window of frames with the

Reprocess HD mode to obtain optimal estimates of six-degree-of-freedom kinematics for each segment (Schepers, et al., 2018).

Linear and angular kinematic data for all surfaces were exported from MVN Analyze at 100 frames per second and imported into Visual3D software (C-Motion, Germantown, Maryland, USA) for additional processing. Center of mass height at each time (COMz) was estimated instantaneously at each time point (t) using segment center of mass vertical positions and masses of the feet, shanks, thighs, pelvis, and trunk. Segment masses and vertical center of mass locations were calculated as proportions of the total body mass and the participant's height (Dempster, 1955; Hanavan Jr, 1964). To account for the mass of the head and arms for which kinematic data were not collected, the segment parameters of the trunk were adjusted to represent the trunk, arms, and head as a rigid unit. The equation used is as follows:

$$COMz(t) = \frac{1}{M}\sum_{i=1}^{N} m_i z_i\,(t) \qquad (1)$$

where M is the total body mass, N is the total number of segments, m_i is the mass of a segment, z_i was the vertical position of the segment center of mass at time point t (Mudie, et al., 2017; Ranavolo, et al., 2008; Saini, et al., 1998).

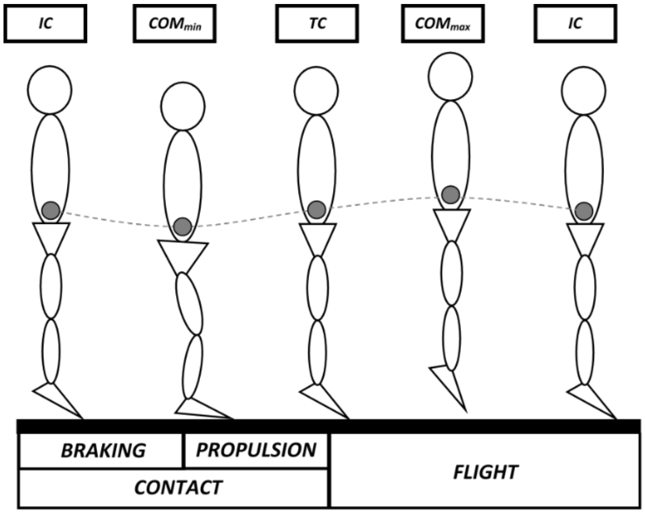

Figure 4.3. Phases, sub-phases, and key events of hopping. IC = initial contact, COM_{min} = center of mass minimum height, TC = terminal contact, COM_{max} = center of max maximum height.

Hopping (Figure 4.3) and running (Figure 4.4) cycles were defined as the time series between the instant of terminal ground contact (i.e., toe off) to the subsequent instance of terminal ground contact for the same foot (Cavagna, et al., 1988; Gutmann and Bertram, 2017; Novacheck, 1998; Serpell, et al., 2012). These cycles were then broken down into two phases—flight phase (or aerial phase) and contact phase (or stance phase). The flight phase of hopping was defined from terminal ground contact to subsequent initial ground contact (Blickhan, 1989; Waxman, et al., 2018). The flight phase of running was defined from terminal ground contact of the non-dominant foot to the subsequent initial ground contact of the dominant foot (Blickhan, 1989; Novacheck, 1998; Padulo, et al., 2014). For hopping and running cycles, contact phase was defined from initial ground contact of the dominant foot to terminal ground contact of the same foot.

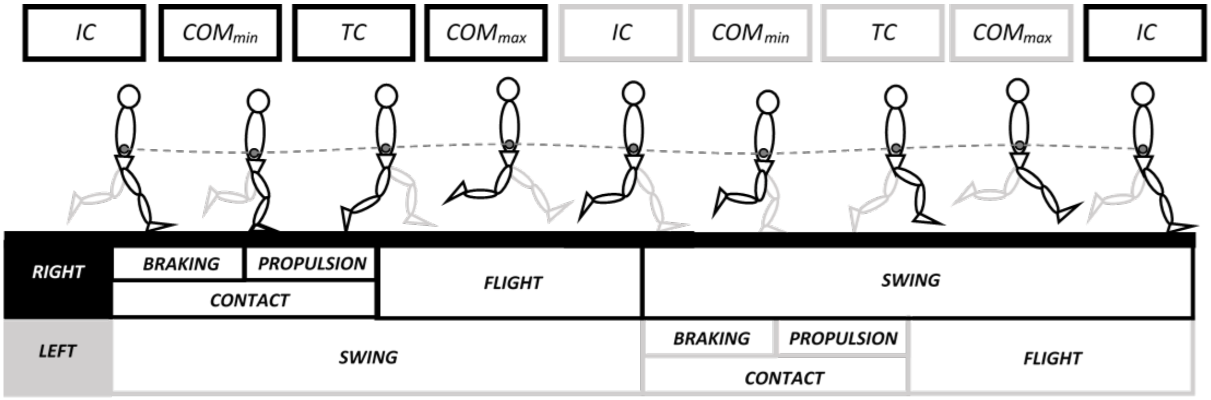

Figure 4.4. Phases, sub-phases, and events of running. IC = initial contact, COM_{min} = center of mass minimum height, TC = terminal contact, COM_{max} = center of max maximum height.

Events delineating the hopping and running phases were created with a pipeline of user-defined peak detection algorithm commands. Local minima in the vertical center of mass position time series were identified as minimum center of mass height (COM_{min}). For the purpose of narrowing the window scanned for ground contact events, local maxima directly proceeding each COM_{min} were identified as maximum center of mass height (COM_{max}). Terminal ground contact events were identified between COM_{min} and COM_{max} as local maxima in the sagittal plane angular velocity time series of the foot. Initial ground contact events were identified between COM_{max} and COM_{min} at local maxima in the resultant linear acceleration time series of the foot. (Bergamini, et al., 2012; Reenalda, et al., 2019; Reenalda, et al., 2016; Sabatini, et al., 2005; Strohrmann, et al., 2012). Following event creation, trials were visually inspected in order to detect any erroneous data or missing events within the hopping or running cycles.

Stiffness measures during hopping and running were computed using the fourth, fifth, and sixth cycles of each trial to eliminate misrepresentative variability caused by movement initiation and termination. For both tasks, vertical stiffness (K_{vert}) was computed as the ratio of peak vertical ground reaction force (peak GRF_{vert}) to center of mass vertical displacement (ΔCoM_{vert}). Leg stiffness (K_{leg}), was also computed during the hopping and running trials. Computationally, the denominator is the only difference between leg stiffness and vertical stiffness. Leg stiffness uses the change in leg length (ΔL_{leg}) from standing length to the maximum shortened length during stance phase instead of ΔCoM_{vert}. The actual maximum shortened leg length during the running trials is typically measured as the distance from the center of pressure location along the foot to the greater trochanter or hip. However since center of pressure data was not measured in this study, the resultant distance from the position of the proximal end of the thigh (representative of the greater trochanter) to distal end of the shank (representative of the lateral malleoli) was used as a surrogate measure during both standing and during the running trials (DuBose, et al., 2017). The locations of segment ends were modeled based on segment lengths calculated as a proportion of total height and the linear positions and relative rotations of the foot, shank, and thigh segments (Drillis, et al., 1969; Schepers, et al., 2018; Winter, 2009).

To estimate peak vertical ground reaction force (*peak* GRF_{vert}), the sine wave method previously validated for both hopping and running for field-based measures (Dalleau, Belli, Viale, Lacour, & Bourdin, 2004; Morin, Dalleau, Kyröläinen, Jeannin, & Belli, 2005) was employed (Appendix A). In this method, *peak* GRF_{vert} is modeled using the following equation:

$$peak\ GRF_{vert} = m \cdot g \cdot \frac{\pi}{2} \cdot \left(\frac{T_f}{T_c} + 1\right) \tag{2}$$

where m is the body mass in kg, g is gravitational acceleration, T_f is flight time, and T_c is contact time. Contact and flight times were defined from initial ground contact to terminal ground contact and terminal ground contact to initial ground contact, respectively.

Using the vertical position of the center of mass estimated using Equation 1, center of mass vertical displacement (ΔCoM_{vert}) was calculated as:

$$\Delta CoM_{vert} = CoM_{vert\_@initial\ ground\ contact} - COM_{vert_{@minimum\ height}} \tag{3}$$

Vertical stiffness (K_{vert}) was then measured during hopping and running using Equation 2 in the numerator and Equation 3 in the denominator:

$$K_{vert} = \frac{peak\ GRF_{vert}}{\Delta CoM_{vert}} \tag{4}$$

During running only, leg stiffness (K_{leg}) was computed as:

$$K_{leg} = \frac{peak\ GRF_{vert}}{\Delta L_{leg}} \tag{5}$$

using Equation 2 in the numerator and the following equation for ΔL_{leg} in the denominator:

$$\Delta L_{leg} = L_{standing} - L_{maximum\ compression} \tag{6}$$

The vertical and leg stiffness values were originally computed in units of N/m but were normalized by body weight (BW) and leg length (L) to account for anthropometric variations between participants. Thus, the stiffness values reported are unitless but should be interpreted as having units of BW/L.

In addition to vertical and leg stiffness, self-selected hopping and stride frequencies were computed. Hop frequency was calculated as the reciprocal of the duration of the hopping cycle (Farley, et al., 1991; Kuitunen, et al., 2011; Mudie, et al., 2017; Ranavolo, et al., 2008). Similarly, stride frequency was computed as the reciprocal of the duration of the running cycle (Cavagna, et al., 1964; Farley and Gonzalez, 1996; Padulo, et al., 2014).

Statistical Analysis.

Data were analyzed using statistical software (SPSS, Version 25.0, SPSS Inc., Chicago, IL, USA). The distribution of the data was assessed with Shapiro-Wilk tests and failed to meet the assumption of normality. Therefore, nonparametric analyses were performed to assess for differences in stiffness and frequency variables among the four turf surfaces. Repeated measures Friedman ANOVA by ranks tests were conducted for vertical and leg stiffness during hopping and running, hopping frequency, and stride frequency. Statistical significance was set a priori at $\alpha = .05$.

Results

No significant differences between turf surfaces were detected for any of the stiffness or frequency measures during hopping and running, $p < .05$. Summary statistics for all hopping and running (Table. 4.2) variables are provided.

Table 4. 2.

Stiffness and frequency parameters of hopping and running

Parameter	*N*	Synthetic Turf 1		Synthetic Turf 2		Synthetic Turf3		Natural Turf		χ^2	*p*-value
		M	(SD)	M	(SD)	M	(SD)	M	(SD)		
Hopping											
Hopping frequency (Hz)	17	1. 97	(0. 20)	1. 94	(0. 19)	1. 97	(0. 19)	1. 96	(0. 20)	2. 434	. 498
Kvert (BW/L)	17	21. 43	(2. 69)	22. 11	(1. 94)	21. 94	(2. 40)	22. 56	(3. 02)	. 607	. 901
Kleg (BW/L)	17	14. 05	(1. 68)	14. 36	(1. 86)	14. 34	(1. 87)	14. 67	(2. 02)	6. 870	0. 74
Running											
Stride frequency (Hz)	17	1. 34	(0. 09)	1. 35	(0. 09)	1. 35	(0. 12)	1. 34	(0. 11)	7. 367	0. 058
Kvert (BW/L)	17	42. 09	(6. 23)	43. 74	(11. 72)	41. 21	(7. 10)	43. 75	(13. 32)	4. 129	0. 256
Kleg (BW/L)	17	25. 84	(3. 57)	26. 04	(3. 99)	25. 36	(4. 27)	27. 51	(3. 70)	6. 035	0. 112

Note. Significance was set at α = . 05. M = Mean, SD = standard deviation, χ^2 = Friedman test statistic. BW/L= bodyweight/leg length

Discussion

Previous studies investigating leg and vertical stiffness during running and hopping on surfaces of varying stiffnesses have demonstrated that vertical stiffness of the surface and lower extremity combined (also termed total vertical stiffness) are maintained across surfaces through adaptations in leg stiffness (Farley, et al., 1998; Ferris and Farley, 1997; Ferris, et al., 1999; Ferris, et al., 1998; Kerdok, et al., 2002). While leg stiffness adjustments between turf surfaces were not detected in the current study, vertical stiffness demonstrated consistency between synthetic and natural turf. When considering this finding in light of known differences in the firmness of these turf surfaces, the findings of this study are in agreement with the literature (Farley, et al., 1998; Ferris and Farley, 1997; Ferris, et al., 1999; Ferris, et al., 1998; Kerdok, et al., 2002) and indicate that participants are able to run and hop on these surfaces using similar movement patterns.

Changes in leg stiffness during bouncing locomotion typically represent functional load attenuations when stiffness is reduced and elastic storage utilization strategies when it is increased (Brazier, et al., 2014). Furthermore, adaptations often manifest as a means of optimizing mechanical efficiency (Kerdok, et al., 2002). In the current study, leg stiffness nor vertical stiffness were changed in response to changes in turf and self-selected hopping and running frequencies were consistent across all surfaces. These findings imply that the body interprets the biomechanical demands of the surfaces to be similar. As suggested by Rennie, Vanrenterghem, Littlewood, & Drust (2016), this mechanical adaptive ability is important for maintaining dynamic stability when running on varied surfaces.

Leg stiffness as measured in the current study did not differ between surfaces. Evidence from investigations of joint stiffness contributions to leg stiffness has called attention to the importance of adjustments at the ankle during hopping and running on different surfaces (Farley, et al., 1998; Farley and Morgenroth, 1999; R. Müller, Grimmer, & Blickhan, 2010). However, the alternative method employed to compute change in leg length leg (i.e., greater trochanter to malleolus) overlooked potential adjustments made at the ankle and foot and is considered a limitation.

Conclusion

The results of this study indicated that vertical stiffness during hopping and running is consistent across synthetic and natural turf surfaces. Additionally, leg stiffness as measured in this study did not differ between surfaces. Though limited, this study offers preliminary evidence in support of previous research regarding the ability of the lower extremity to account for surface stiffness and effectively maintain a consistent total vertical stiffness. To build towards a better understanding of the influence of synthetic and natural turf on the contributions of stiffness to performance and safety, future research should include both submaximal and maximal-effort locomotive tasks in the analyses.

CHAPTER 5

Inter-segmental coordination variability during hopping and running on natural and synthetic turf surfaces

Keywords: Coordination, movement variability, locomotion, synthetic turf, natural turf

Introduction

Athletes exhibiting coordinated movement patterns and consistent performance can achieve a directed outcome by continually adjusting to changes in the task, organismic, and environmental constraints (Davids, et al., 2003; Newell, 1986). This ability is acquired through extensive practice and exposure to diverse performance parameters, including different playing surfaces. Furthermore, an athlete's adaptability is characterized by functional variations in efficient and effective movement patterns as a response to varying performance parameters. (Davids, et al., 2003; Glazier, et al., 2003; Riley and Turvey, 2002; Sánchez et al., 2017; Seifert, et al., 2013; Seifert, Komar, Crettenand, & Millet, 2014).

Athletes considered to be skilled at a certain task are able to achieve desired movement outcomes by demonstrating a range of optimized and adaptive movement patterns. These movement patterns properly organize the degrees of freedom of the musculoskeletal system, to adjust to changes in environmental conditions (Davids, et al., 2015; Davids, et al., 2006; Davids and Glazier, 2010; Hamill, et al., 2012; Newell, 1985; Rosalie and Müller, 2012). Thus expert coordination emerges as flexible yet stable—flexible in its use of controlled variations of the different coordinated degrees of freedom and stable, but not rigid, in its ability to efficiently produce effective outcomes through a multitude of motor options (Glazier, et al., 2003; Riley and Turvey, 2002; Seifert, et al., 2013; Seifert, et al., 2014).

While a certain range of inter-segmental coordination variability is considered to be necessary for carrying out coordinated movements with high efficacy and efficiency, an ideal range is also believed to be related to healthy, functional movements (Hamill, et al., 2006; Stergiou and Decker, 2011). Multiple studies involving different movement tasks have observed reduced amounts of coordination variability between relative segments in individuals who have been injured or are experiencing pain in comparison to non-injured and pain-free controls (Drewes, et al., 2009; Kurz, et al., 2005; Miller, et al., 2008; Nematollahi, et al., 2016; Seay, et al., 2011). This decrease in coordination variability is thought to be an adaptive mechanism for avoiding coordination patterns that further engage damaged tissues or cause discomfort (Bartlett, Wheat, & Robins, 2007). Though largely anecdotal at this time, repetitive execution of a less variable coordination pattern in healthy individuals is thought to imply an increased risk of overuse injuries and damage to tendons, ligaments, and cartilage involved in the acting movement system. This is believed to occur after exposure to harmful cumulative loads resulting from insufficient distribution of stresses across the involved passive, soft tissues (Bartlett, et al., 2007; Hamill, et al., 2012).

An athlete's performance and musculoskeletal health hinges on their ability to exploit the abundant degrees of freedom in the body and adapt their movement patterns when faced with changes in environmental constraints. Some of the environmental constraints imposed are derived from physical properties of the playing surface, such as firmness and traction. However, research has yet to offer a thorough understanding of the biomechanical response of athletes to synthetic and turf surfaces and whether coordination variability is adjusted as a result

(Charalambous, et al., 2016). Therefore, the purpose of this study was to investigate lower extremity inter-segmental coordination variability in athletes during two fundamental sport-related tasks, hopping and running, on four turf surfaces—three synthetic turf surfaces and one natural turf surface (Table 5.1). Various non-linear methods for quantifying inter-segmental coordination variability during cyclical movements have been employed throughout the literature (Glazier, et al., 2003; Komar, et al., 2015; Miller, et al., 2010). However since the energy-returning functions of elastic components within the musculoskeletal system during hopping and running are bound by temporally-influenced properties (Wilson and Lichtwark, 2011), continuous relative phase analysis (CRP) was selected to characterize coordination variability as it incorporates both spatial and temporal data. This analysis depicts segment coupling coordination during movement cycles as the difference between velocity-displacement phase angles of relative paired segments over time (Glazier, et al., 2003; Hein, et al., 2012). Interestingly, such an approach has yet to be utilized in research investigating athlete biomechanics on natural versus synthetic turf and provides a means for evaluating the flexibility of coordination patterns demonstrated by the lower extremity linked-segment system. It was hypothesized that inter-segmental coordination variability would be greatest of natural turf and progressively reduced on synthetic turf 3, synthetic turf 2, and synthetic turf 1, respectively.

Methods

Participants.

To determine the sample size needed for this study, an a priori power analysis was conducted in G*Power (Version 3.1.9.2) with the parameter set as follows: power of 0.80, a type I error rate threshold of 0.05, a medium effect size of 0.25, a correlation coefficient between

Table 5.3.

Turf System Specifications of Each Testing Surface

	Fiber Type	Pile Height (in)	Shock Pad (mm)	Infill Composition	Face Weight (oz/yd$^{2)}$	Firmness (mm)
Synthetic Turf 1	Dual Fiber Hybrid (slit-film fiber and monofilament fiber)	2.25 in	None	60% sand, 40% rubber	46	5.65
Synthetic Turf 2	Dual Fiber Hybrid (slit-film fiber and monofilament fiber)	2.0 in	14 mm	60% sand, 40% rubber	46	6.66
Synthetic Turf 3	Dual Fiber Hybrid (slit-film fiber and monofilament fiber)	1.75 in	14 mm	90% coconut husk/fibers, 10% naturally derived plant-based matter	46	6.89
	Grass Type	Height of Cut (in)		Soil Composition		
Natural Turf	Tifway Bermudagrass	5/8 in		Loamy sand, 2.1% organic matter		7.04

Note. Firmness represents surface deformation.

repeated measures of 0.70, and a nonsphericity correction of 1. The results of this analysis suggested a sample size of 15. Seventeen participants (age: 23.1 ± 2.9 years; height: 1.81 ± 0.06 m; mass: 77.8 ± 9.9 kg) were recruited from the surrounding community for the study. Prior to participation, all participants indicated their voluntary involvement by signing an informed consent for this study as approved by the university Institutional Review Board. Participants completed a health-history questionnaire to determine eligibility in this study. Inclusion criteria included healthy males who participate in a minimum of three days of moderate to vigorous and had at least two years of high school athletic experience. Individuals with a current or recent lower extremity injury (i.e., within the last three months), prior lower extremity injury that required surgery, or an allergy to adhesive were excluded from participation.

Design and Protocol.

In order to determine the influence of different turf surfaces on select biomechanical movement variables, we chose to test four different turf surfaces—three synthetic turf surfaces and one natural turf surface (Table 5.1). To reduce the risk of fatigue, data collection was split into two sessions held on separate days with two of the four surfaces tested per session. The surface testing order was determined per participant by random selection of a starting point within the following cyclic order of test surfaces: synthetic turf 1, synthetic turf 2, synthetic turf 3, and natural turf.

Since data collection took place at an outdoor turf field laboratory, there were certain conditions that could not be controlled for, but actions were taken to reduce their influence on the testing environment. Surface and ambient temperatures were not controlled for, but both days of data collection for every participant took place at the same general time of day (i.e., either in early morning, late morning, midday, early afternoon, or late afternoon). Additionally, surface moisture content was not controlled. However, to avoid the influence of excessive moisture, data collections did not take place after rainfall until a full day had passed.

Upon arriving at the outdoor turf field laboratory, participants' height, mass, and foot length measurements were recorded and they were fitted with a new pair of cleats to be worn during the study. Substantial evidence has demonstrated the complexity of the cleat-ground interface and revealed that various elements of cleat design, such as stud configuration and shape, upper, heel cup, and shoe plate stiffness are known to influence the shoe-ground interaction (Clarke and Carré, 2010; Hennig and Sterzing, 2010; Kulessa, et al., 2017; C. Müller, T. Sterzing, M. Lake, et al., 2010; C. Müller, T. Sterzing, J. Lange, et al., 2010; Schrier, et al., 2014; Severn, et al., 2008; Silva, et al., 2017). Thus to minimize potential variations induced by differences in cleat models across participants, each individual wore one of two provided models (Figure 5.1). Both models had the same upper, heel, and shoe plate construction including stud configuration and differed in mass by less than 1 g.

Figure 5.1. Cleat models used in this study. (A) Under Armour Speedform® MC, (B) Under Armour Spotlight.

Eight wireless inertial measurement unit (IMU) sensors (MTw, Xsens Technologies B.V., Enschede, the Netherlands) were affixed bilaterally, to the feet, lower legs, thighs, as well as to the pelvis, and trunk (Figure 5.2). To ensure the sensors were firmly affixed yet not restricting movement, the foot trackers were secured to the top of the cleats with athletic tape and the remaining sensors were attached directly to the skin with elastic adhesive bandage (Cover-Roll™; BSN Medical, Beiersdorf AG, Hamburg, Germany). Shank and thigh sensors were further secured with foam prewrap (Z – wrap, Johnson & Johnson, Langhorne, PA, USA). Sensor-to-segment calibration was then carried out by having the participant assume a static neutral pose, walk forward approximately 3 meters from the location of the static pose, and then walk back to the same location and resume a static neutral pose (Xsens, MVN MTw User Manual, 2018).

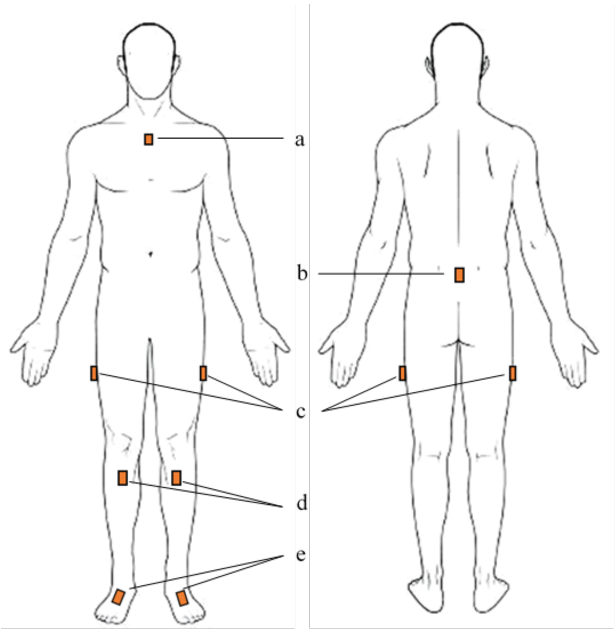

Figure 5.2. IMU sensor placement based on Xsens MVN MTw User Manual (2018). (a) Trunk Sensor – sternum just below the sternal angle, (b) Pelvis Sensor– sacral bone between left and right iliac spine, (c) Thigh Sensors – lateral thigh midway between greater trochanter and lateral femoral epicondyle, (d) Shank Sensors – flat surface medial to the tibial tuberosity, (e) Foot Sensors – Dorsal surface just distal to the navicular.

Prior to testing, each participant was allotted unlimited time to perform their typical individual warm-up routine. For both data collection days, warm-up routines lasted 10 minutes on average and included light jogging, static and dynamic lower extremity stretches, and short distance runs. On each of the four turf surfaces, participants performed three trials of a single leg hopping task and a submaximal 35-m running task. The task order was randomized for each participants and each surface. For the single leg hopping trials, participants were instructed to hop in place ten times at a steady self-selected frequency on their dominant limb and with their hands resting on their hips. Leg dominance was defined as the leg identified by each participant as his preferred kicking leg (Granata, et al., 2002; Hobara, et al., 2010; Mudie, et al., 2017; Padua, et al., 2006). For the 35-m submaximal running trials, the participants were instructed to run the set distance at a steady, submaximal, self-selected frequency. Since constraining movement frequencies to a target pace is known to influence movement parameters (Auyang, Yen, & Chang, 2009; Hobara et al., 2010), self-selected frequencies for both tasks were chosen in order to measure the participant's authentic, unaltered response to each surface.

Data Acquisition and Processing.

Synchronized three-dimensional accelerometer, gyroscope, and magnetometer signals internally sampled at >1000 Hz by each IMU sensor were transferred wirelessly amongst each other as well as the Awinda base station connected to the data collection workstation. Using the Xsens MVN Analyze software engine (Version 2019.0, Enschede, the Netherlands), the sampled signals from each sensor were processed frame-by-frame using advanced sensor fusion algorithms and advanced biomechanical models, resulting in stable motion tracking at a rate of 100 Hz. After each trial, data were reprocessed over a larger window of frames with the Reprocess HD mode to obtain optimal estimates of six-degree-of-freedom kinematics for each segment (Schepers, et al., 2018).

Linear and angular kinematic data for all surfaces were exported from MVN Analyze at 100 frames per second and imported into Visual3D software (C-Motion, Germantown, Maryland, USA) for additional processing. Center of mass height at each time (COMz) was estimated instantaneously at each time point (t) using segment center of mass vertical positions and masses of the feet, shanks, thighs, pelvis, and trunk. Segment masses and vertical center of mass locations were calculated as proportions of the total body mass and the participant's height (Dempster, 1955; Hanavan Jr, 1964). To account for the mass of the head and arms for which kinematic data were not collected, the segment parameters of the trunk were adjusted to represent the trunk, arms, and head as a rigid unit. The equation used is as follows:

$$COMz(t) = \frac{1}{M}\sum_{i=1}^{N} m_i z_i\,(t) \qquad (1)$$

where M was the total body mass, N was the total number of segments, m_i was the mass of a segment, z_i was the vertical position of the segment center of mass at time point t (Mudie, et al., 2017; Ranavolo, et al., 2008; Saini, et al., 1998).

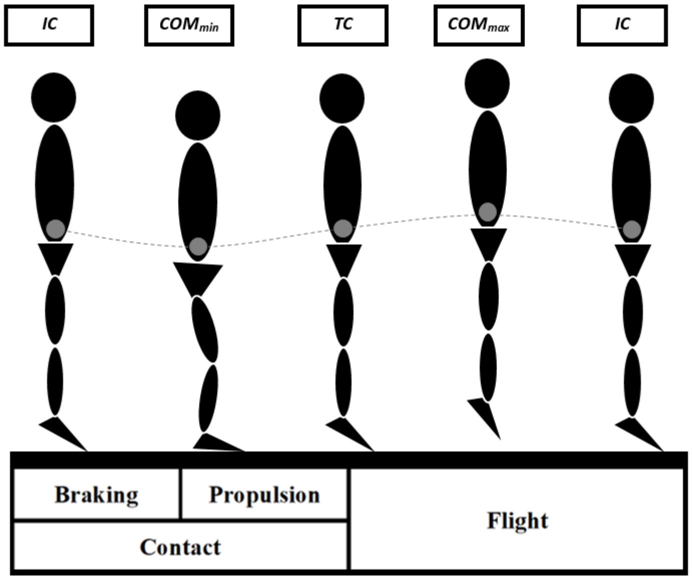

Figure 5.3. Phases, sub-phases, and key events of hopping. IC = initial contact, COM$_{min}$ = center of mass minimum height, TC = terminal contact, COM$_{max}$ = center of max maximum height.

Hopping (Figure 5.3) and running (Figure 5.4) cycles were defined as the time series between the instant of terminal ground contact (i.e., toe off) to the subsequent instance of terminal ground contact for the same foot (Cavagna, et al., 1988; Gutmann and Bertram, 2017; Novacheck, 1998; Serpell, et al., 2012). These cycles were then broken down into two phases—flight phase (or aerial phase) and contact phase (or stance phase). The flight phase of hopping was defined from terminal ground contact to subsequent initial ground contact (Blickhan, 1989; Waxman, et al., 2018). The flight phase of running was defined from terminal ground contact of the non-dominant foot to the subsequent initial ground contact of the dominant foot (Blickhan, 1989; Novacheck, 1998; Padulo, et al., 2014). For hopping and running cycles, contact phase was defined from initial ground contact of the dominant foot to terminal ground contact of the same foot.

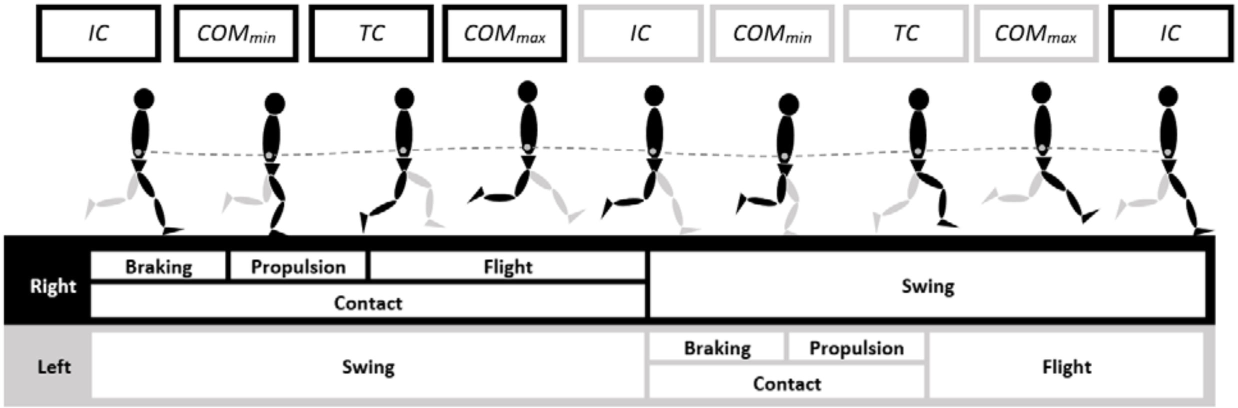

Figure 5.4. Phases, sub-phases, and events of running. IC = initial contact, COM_{min} = center of mass minimum height, TC = terminal contact, COM_{max} = center of max maximum height.

The contact phases of running and hopping were divided into two sub-phases of interest— braking and propulsion. Typically, the instant of peak vertical ground reaction force marks the transition from braking to propulsion (Caderby and Dalleau, 2018; Cavagna, et al., 1964; Kuitunen, et al., 2011; Ranavolo, et al., 2008). Whole body center of mass minimum height (*COMmax*) was also observed at this point of the contact phase (Brughelli and Cronin, 2008; Buchheit, et al., 2015; Caderby and Dalleau, 2018; Ferris and Farley, 1997) (Figure 5.5). Since ground reaction forces were not directly measured in this study, the braking sub-phase was alternatively defined from initial ground contact to the instant of maximum center of mass vertical displacement, and the propulsion sub-phase defined from instant of maximum center of mass vertical displacement to terminal ground contact. Initial contact and terminal ground contact events were created with user-defined peak detection pipeline commands that automatically identified distinctive local maxima in the resultant linear acceleration and angular velocity magnitudes of the foot, respectively (Bergamini, et al., 2012; Reenalda, et al., 2019; Reenalda, et al., 2016; Sabatini, et al., 2005; Strohrmann, et al., 2012).

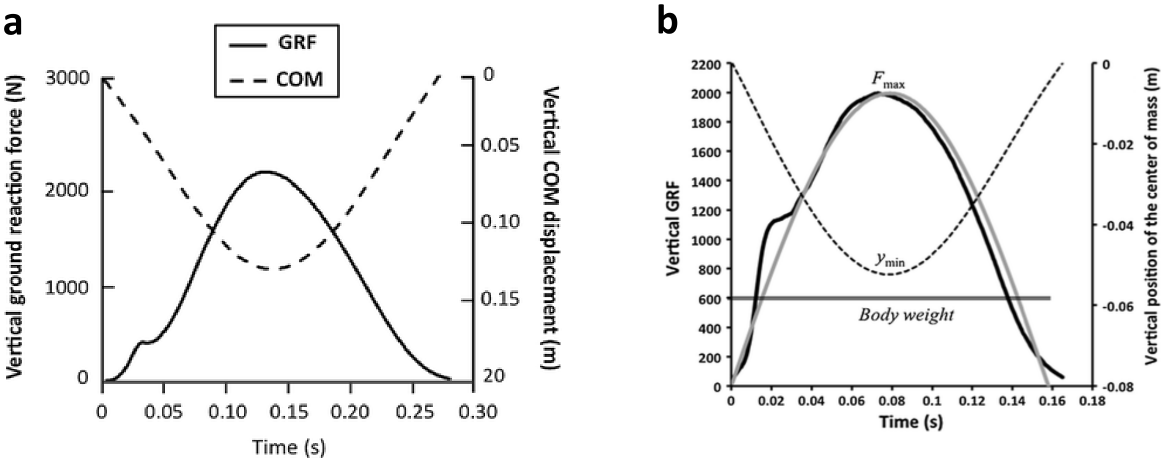

Figure 5.5. Concurrent timing of peak vertical ground reaction force and maximum vertical center of mass displacement during: (a) hopping [Adapted from Caderby and Dalleau (2018)] and (b) running [Adapted from Morin (2018)].

Events delineating the hopping and running phases and sub-phases of interest were created with a pipeline of user-defined peak detection algorithm commands. Local minima in the vertical center of mass position time series were identified as minimum center of mass height (*COMmin*). For the purpose of narrowing the window scanned for ground contact events, local maxima directly proceeding each COM_{min} were identified as maximum center of mass height (COM_{max}). Terminal ground contact events were identified between COM_{min} and COM_{max} as local maxima in the sagittal plane, angular velocity time series of the foot. Initial ground contact events were identified between COM_{max} and COM_{min} at local maxima in the resultant linear acceleration time series of the foot. (Bergamini, et al., 2012; Reenalda, et al., 2019; Reenalda, et al., 2016; Sabatini, et al., 2005; Strohrmann, et al., 2012). Following event creation, trials were visually inspected in order to detect any erroneous data or missing events within the hopping or running cycles.

Absolute segment angular displacements were computed relative to the right horizontal of global sagittal and frontal planes (Figure 5.6). Afterward, absolute segment angular velocities were computed as the first derivative of the segment angular displacements. To ensure steady movement, time series data for these parameters were sampled during the braking and propulsion sub-phases for only the fourth, fifth, and sixth hopping and running cycles of each trial. Braking and propulsion data samples were then extrapolated to 101 data points to enable mean ensemble data to be calculated at 1% intervals (Smallmana, et al., 2013).

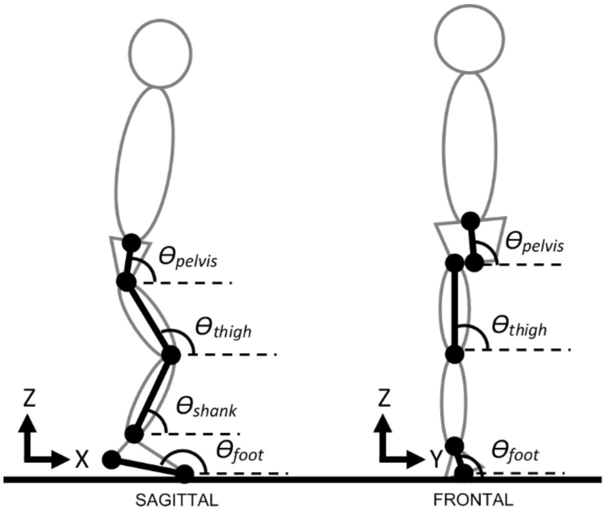

Figure 5.6. Absolute segment angles computed relative to the global sagittal and frontal planes.

Extrapolated segment angular displacement and angular velocity data from each braking and propulsion sample of each trial were exported to MATLAB® for additional processing (R2016a, Mathworks, Inc., Natick, MA). Using custom code, the following procedures were carried out for the hopping and running braking and propulsion sub-phases separately and for each turf to compute CRP variability for the following segment couplings of interest: pelvis-thigh, thigh-shank, thigh-foot, and shank-foot sagittal plane couplings and pelvis-thigh and thigh-foot frontal plane couplings. Two normalization procedures were employed in order to account for individual frequency and amplitude variations. These procedures also ensured that a normalized angular displacement value of zero represents the midpoint of the dynamic range of motion and an angular velocity value of zero continues to represent no change in angular displacement occurring at that time point (Hamill, et al., 1999; Lamb and Stöckl, 2014; Miller, et al., 2010; Miller, et al., 2008; Peters, et al., 2003; Prejean and Ricard, 2019). Angular displacements (θ) were normalized per trial by setting the minimum angle at −1, the maximum angle as 1, and midpoint at 0:

$$\theta_{i,norm} = \frac{2*[\theta_i - \min(\theta)]}{\max(\theta) - \min(\theta)} - 1 \qquad (2)$$

where *i* represents each of the 101 data points in the time series (Hamill, et al., 1999). Angular velocities (ω) were normalized per trial by setting the absolute maximum angular velocity of the time series as ±1:

$$\omega_{i,norm} = \frac{\omega_i}{\max(|\omega|)} \qquad (3)$$

Using the normalized angular displacement and velocity data for each segment, phase angles (φ) were calculated between -180° and 180° at each point in the time series:

$$\varphi_i = \tan^{-1}\left(\frac{\omega_{i,norm}}{\theta_{i,norm}}\right) \tag{4}$$

From these phase angles, relative phase angles (Φ) for each of the segment couplings of interest were computed at each point of the time series by subtracting the phase angle of the distal segment from the phase angle of the proximal segment:

$$\Phi = \varphi_{proximal} - \varphi_{distal} \tag{5}$$

The relative phase angles at each point of the time series were averaged across all samples from all trials (N=12 per participant) to generate mean ensemble CRP angles and standard deviations. The standard deviations of the ensemble CRP angles across all 101 data points were averaged to quantify CRP variability:

$$CRPvariability = \frac{\sum_{i=1}^{N} SD_i}{N} \tag{6}$$

The outcome of these computations is a single CRP variability value that is representative of the average amount of coordination variability observed.

Statistical Analysis.

Data were analyzed using statistical software (SPSS, Version 25.0, SPSS Inc, Chicago, IL, USA). The distribution of the data was assessed with Shapiro-Wilk tests and failed to meet the assumption of normality. Therefore, nonparametric analyses were performed to assess for differences in CRP variability among the four turf surfaces. Repeated measures Friedman ANOVA by ranks tests were conducted for each segment coupling pair during the braking and propulsion sub-phases of hopping and running. Statistical significance was set a priori at $\alpha = .05$.

Results

A significant effect of turf on the CRP variability of the pelvis-thigh sagittal plane coupling during the braking sub-phase of hopping was detected, $\chi^2(3) = 8.365$ $p = .037$. Dunn's pairwise post hoc analyses with a Bonferroni correction for multiple comparisons were carried out and determined that CRP variability of the pelvis-thigh sagittal plane coupling was significantly less on synthetic turf 1 than on natural turf (55.3° ± 16.8° vs. 67.1° ± 17.2°, $p = .03$, $W = .16$). Differences in CRP variability during the braking sub-phase of hopping for the five other couplings were not statistically significant between turf surfaces, $p <.05$ (Table 5.2). Additionally, no significant differences in CRP variability between turf surfaces were detected for any of the couplings during the propulsion sub-phase of hopping (Table 5.2) nor during the braking and propulsion sub-phase of running, $p < .05$. (Table 5.3).

Discussion

By examining well-learned fundamental movements that did not entail maximal-effort or extrinsically regulated task demands (i.e., sub-maximal, self-paced hopping and running), it was expected that differences in coordination variability as measured by CRP variability of inter-segmental couplings would be observed. Contrary to these hypotheses, no differences in CRP variability between turf surfaces were found for any of the segment couplings during hopping and running, except for one. The single significant finding was observed during the braking sub-phase of hopping, which is when the body is tasked with resisting downward acceleration of the center of mass. Specifically, the sagittal plane pelvis-thigh coupling demonstrated significantly less CRP variability on synthetic turf 1 compared to natural turf.

Movement patterns that allow for greater but not excessive variability between segments are widely considered to be a healthier, more flexible display of adaptive coordination than movement patterns with less variability (Davids, et al., 2003). Observations of a reduction in variability may place that system at greater risk of injury due to repetitive stress being applied to

Table 5.2.

Continuous relative phase (CRP) variability (°) during the braking and propulsion sub-phases of hopping

			Synthetic Turf 1	Synthetic Turf 2	Synthetic Turf 3	Natural Turf		
Coupling		*N*	M (SD)	M (SD)	M (SD)	M (SD)	χ^2	*p*-value
Braking	*Sagittal Plane*							
	Pelvis-Thigh	17	55.3 (16.8)[ǂ]	61.5 (13.8)	63.5 (17.9)	67.1 (17.2)	8.365	.037*
	Thigh-Shank	17	55.0 (18.5)	45.0 (17.9)	55.2 (21.7)	56.8 (19.3)	4.412	.230
	Thigh-Foot	17	58.0 (21.8)	53.3 (19.5)	64.4 (24.1)	65.1 (21.2)	4.553	.216
	Shank-Foot	17	26.3 (10.0)	28.3 (14.8)	30.9 (17.2)	29.0 (16.1)	1.871	.615
	Frontal Plane							
	Pelvis-Thigh	17	67.2 (23.3)	71.4 (23.6)	69.6 (20.9)	67.9 (24.0)	1.165	.780
	Thigh-Foot	17	52.2 (25.9)	49.1 (25.0)	52.4 (25.2)	53.2 (26.6)	1.871	.615
Propulsion	*Sagittal Plane*							
	Pelvis-Thigh	17	68.6 (17.4)	64.7 (14.4)	65.2 (18.1)	70.0 (23.5)	2.859	.433
	Thigh-Shank	17	60.2 (19.4)	54.1 (16.1)	52.7 (23.6)	61.9 (25.4)	1.871	.615
	Thigh-Foot	17	68.8 (20.3)	63.6 (18.7)	63.6 (27.5)	73.7 (26.9)	6.106	.107
	Shank-Foot	17	27.6 (16.8)	30.2 (20.4)	24.4 (19.0)	27.4 (16.3)	1.871	.615
	Frontal Plane							
	Pelvis-Thigh	17	54.7 (25.5)	56.8 (25.1)	53.2 (25.5)	53.6 (28.5)	4.694	.193
	Thigh-Foot	17	59.8 (32.3)	60.1 (30.7)	64.2 (32.7)	61.8 (36.0)	2.435	.502

Note. Significance was set at α = .05. M = Mean, SD = standard deviation, χ^2 = Friedman test statistic.
*p < .05
[ǂ] Significantly different than natural turf.

Table 5.3.

Continuous relative phase (CRP) variability (°) during the braking and propulsion sub-phases of running.

	Coupling	*N*	Synthetic Turf 1 M (SD)	Synthetic Turf 2 M (SD)	Synthetic Turf 3 M (SD)	Natural Turf M (SD)	χ^2	*p*-value
Braking	*Sagittal Plane*							
	Pelvis-Thigh	17	53.1 (23.7)	51.7 (26.0)	59.1 (21.0)	55.3 (23.2)	1.729	.651
	Thigh-Shank	17	45.6 (21.8)	44.2 (18.5)	52.1 (17.6)	53.8 (18.9)	6.106	.107
	Thigh-Foot	17	66.9 (23.4)	65.7 (20.7)	66.4 (24.1)	69.1 (20.3)	0.741	.876
	Shank-Foot	17	71.5 (25.7)	73.3 (27.8)	75.3 (29.2)	76.8 (22.2)	2.153	.555
	Frontal Plane							
	Pelvis-Thigh	17	69.5 (23.5)	73.2 (21.6)	73.9 (23.5)	71.5 (25.2)	1.518	.687
	Thigh-Foot	17	41.4 (27.7)	42.5 (22.7)	41.3 (24.8)	40.9 (26.5)	1.518	.687
Propulsion	*Sagittal Plane*							
	Pelvis-Thigh	17	75.1 (15.1)	74.4 (21.9)	68.1 (25.9)	69.6 (24.4)	1.024	.816
	Thigh-Shank	17	77.4 (19.9)	75.0 (27.1)	74.3 (32.8)	76.0 (28.8)	3.424	.347
	Thigh-Foot	17	82.4 (16.3)	84.0 (19.0)	78.5 (26.7)	79.0 (25.8)	0.459	.934
	Shank-Foot	17	28.4 (16.1)	32.7 (23.4)	28.0 (22.9)	28.7 (18.2)	2.576	.478
	Frontal Plane							
	Pelvis-Thigh	17	67.8 (21.9)	69.7 (21.7)	69.4 (21.3)	71.3 (18.0)	0.388	.951
	Thigh-Foot	17	41.9 (19.6)	40.8 (21.3)	41.1 (19.4)	34.4 (17.0)	2.012	.591

Note. Significance was set at α = .05. M = Mean, SD = standard deviation, χ^2 = Friedman test statistic.
$^*p < .05$

the same tissues (Hamill, et al., 1999). Evidence of reduced coordination variability in the pelvis-thigh sagittal plane coupling was found in a study comparing CRP measures in people with and without chronic low back pain during free-speed walking (Ebrahimi, et al., 2017). Though not directly observed as a symptom of chronic low back pain and not the cause, the author suggested that a less variable coordination pattern may be indicative of a reduced ability to absorb shock and may lead to further injury (Ebrahimi, et al., 2017; Stergiou, Jensen, Bates, Scholten, & Tzetzis, 2001). Given that low back pain is commonly reported in athletes after playing on synthetic turf (Aoki et al., 2010; Bianco et al., 2016), the reduced coordination variability in the pelvis-thigh sagittal coupling observed on the firmest of the synthetic turfs tested in this study, warrants attention and should be investigated further. The events considered in this project focused on the intervals loading. Future research should consider the different alignments employed between the trunk, pelvis, and thigh to ascertain whether the altered postures place a greater demand on the trunk extensors.

Conclusion

The results of this study demonstrated that coordination variability between relative segments, in the dominant limb, is largely unaffected by different turf surfaces. However, the significant reduction in variability observed between the pelvis and thigh may indicate an adverse alternative movement pattern during the braking sub-phase of hopping and warrants attention. Future investigation into this is suggested, especially regarding firm synthetic turf systems that do not include a shock pad.

REFERENCES

Andersson, H., Ekblom, B., & Krustrup, P. (2008). Elite football on artificial turf versus natural grass: movement patterns, technical standards, and player impressions. *Journal of Sports Sciences, 26*(2), 113-122.

Aoki, H., Kohno, T., Fujiya, H., Kato, H., Yatabe, K., Morikawa, T., & Seki, J. (2010). Incidence of injury among adolescent soccer players: a comparative study of artificial and natural grass turfs. *Clinical Journal of Sport Medicine, 20*(1), 1-7.

Arampatzis, A., De Monte, G., Karamanidis, K., Morey-Klapsing, G., Stafilidis, S., & Brüggemann, G.-P. (2006). Influence of the muscle-tendon unit's mechanical and morphological properties on running economy. *Journal of Experimental Biology, 209*(17), 3345-3357.

Auyang, A. G., Yen, J. T., & Chang, Y.-H. (2009). Neuromechanical stabilization of leg length and orientation through interjoint compensation during human hopping. *Experimental Brain Research, 192*(2), 253-264.

Bartlett, R., Wheat, J., & Robins, M. (2007). Is movement variability important for sports biomechanists? *Sports Biomechanics, 6*(2), 224-243.

Bergamini, E., Picerno, P., Pillet, H., Natta, F., Thoreux, P., & Camomilla, V. (2012). Estimation of temporal parameters during sprint running using a trunk-mounted inertial measurement unit. *Journal of Biomechanics, 45*(6), 1123-1126.

Bernstein, N. A. (1967). *The coordination and regulation of movements* Oxford: Pergamon Press.

Bianco, A., Spedicato, M., Petrucci, M., Messina, G., Thomas, E., Sahin, F. N., . . . Palma, A. (2016). A prospective analysis of the injury incidence of young male professional football players on artificial turf. *Asian Journal of Sports Medicine, 7*(1), 1-6.

Blickhan, R. (1989). The spring-mass model for running and hopping. *Journal of Biomechanics, 22*(11-12), 1217-1227.

Blum, Y., Lipfert, S. W., & Seyfarth, A. (2009). Effective leg stiffness in running. *Journal of Biomechanics, 42*(14), 2400-2405.

Brazier, J., Bishop, C., Simons, C., Antrobus, M., Read, P. J., & Turner, A. N. (2014). Lower extremity stiffness: Effects on performance and injury and implications for training. *Strength & Conditioning Journal, 36*(5), 103-112.

Brughelli, M., & Cronin, J. (2008). Influence of running velocity on vertical, leg and joint stiffness. *Sports Medicine, 38*(8), 647-657.

Buchheit, M., Gray, A., & Morin, J.-B. (2015). Assessing stride variables and vertical stiffness with GPS-embedded accelerometers: preliminary insights for the monitoring of neuromuscular fatigue on the field. *Journal of Sports Science & Medicine, 14*(4), p 698.

Butler, R. J., Crowell III, H. P., & Davis, I. M. (2003). Lower extremity stiffness: implications for performance and injury. *Clinical Biomechanics, 18*(6), 511-517.

Caderby, T., & Dalleau, G. (2018). A Simple Method for Measuring Lower Limb Stiffness in Hopping *Biomechanics of Training and Testing* (pp. 121-138): Springer.

Cavagna, G., Franzetti, P., Heglund, N., & Willems, P. (1988). The determinants of the step frequency in running, trotting and hopping in man and other vertebrates. *The Journal of Physiology, 399*(1), 81-92.

Cavagna, G., Saibene, F., & Margaria, R. (1964). Mechanical work in running. *Journal of Applied Physiology, 19*(2), 249-256.

Cazzola, D., Pavei, G., & Preatoni, E. (2016). Can coordination variability identify performance factors and skill level in competitive sport? The case of race walking. *Journal of Sport and Health Science, 5*(1), 35-43.

Charalambous, L., und Wilkau, H. C. v. L., Potthast, W., & Irwin, G. (2016). The effects of artificial surface temperature on mechanical properties and player kinematics during landing and acceleration. *Journal of Sport and Health Science, 5*(3), 355-360.

Chiu, S.-L., Chang, C.-C., & Chou, L.-S. (2015). Inter-joint coordination of overground versus treadmill walking in young adults. *Gait & Posture, 41*(1), 316-318.

Choi, S. M., Sum, K. W. R., & Leung, F. L. E. (2015). Comparison between Natural Turf and Artificial Turf on Agility Performance of Rugby Union Players. *Advances in Physical Education, 5*(04), 273.

Clarke, J., & Carré, M. (2010). Improving the performance of soccer boots on artificial and natural soccer surfaces. *Procedia Engineering, 2*(2), 2775-2781.

Davids, K., Araújo, D., Seifert, L., & Orth, D. (2015). An ecological dynamics perspective. *Routledge Handbook of Sport Expertise*, 130-144.

Davids, K., Button, C., Araújo, D., Renshaw, I., & Hristovski, R. (2006). Movement models from sports provide representative task constraints for studying adaptive behavior in human movement systems. *Adaptive Behavior, 14*(1), 73-95.

Davids, K., & Glazier, P. (2010). Deconstructing neurobiological coordination: the role of the biomechanics-motor control nexus. *Exercise and Sport Sciences Reviews, 38*(2), 86-90.

Davids, K., Glazier, P., Araujo, D., & Bartlett, R. (2003). Movement systems as dynamical systems. *Sports Medicine, 33*(4), 245-260.

Dempster, W. T. (1955). *Space requirements of the seated operator, geometrical, kinematic, and mechanical aspects of the body with special reference to the limbs*. Michigan State University, East Lansing, MI.

Devita, P., & Skelly, W. A. (1992). Effect of landing stiffness on joint kinetics and energetics in the lower extremity. *Medicine and Science in Sports and Exercise, 24*(1), 108-115.

Diedrichsen, J., Shadmehr, R., & Ivry, R. B. (2010). The coordination of movement: optimal feedback control and beyond. *Trends in Cognitive Sciences, 14*(1), 31-39.

Dragoo, J. L., & Braun, H. J. (2010). The effect of playing surface on injury rate. *Sports Medicine, 40*(11), 981-990.

Drewes, L. K., McKeon, P. O., Paolini, G., Riley, P., Kerrigan, D. C., Ingersoll, C. D., & Hertel, J. (2009). Altered ankle kinematics and shank-rear-foot coupling in those with chronic ankle instability. *Journal of Sport Rehabilitation, 18*(3), 375-388.

Drillis, R., Contini, R., & Bluestein, M. (1969). *Body segment parameters*: New York University, School of Engineering and Science.

DuBose, D. F., Herman, D. C., Jones, D. L., Tillman, S. M., Clugston, J. R., Pass, A., . . . Chmielewski, T. L. (2017). Lower extremity stiffness changes following concussion in collegiate football players. *Medicine and Science in Sports and Exercise, 49*(1), p 167.

Dufek, J. S., & Bates, B. T. (1990). The evaluation and prediction of impact forces during landings. *Medicine and Science in Sports and Exercise, 22*(3), 370-377.

Ebrahimi, S., Kamali, F., Razeghi, M., & Haghpanah, S. A. (2017). Comparison of the trunk-pelvis and lower extremities sagittal plane inter-segmental coordination and variability during walking in persons with and without chronic low back pain. *Human Movement Science, 52*, 55-66.

Ekstrand, J., Hägglund, M., & Fuller, C. (2011). Comparison of injuries sustained on artificial turf and grass by male and female elite football players. *Scandinavian Journal of Medicine & Science in Sports, 21*(6), 824-832.

Ekstrand, J., Timpka, T., & Hägglund, M. (2006). Risk of injury in elite football played on artificial turf versus natural grass: a prospective two-cohort study. *British Journal of Sports Medicine, 40*(12), 975-980.

Farley, C. T., Blickhan, R., Saito, J., & Taylor, C. R. (1991). Hopping frequency in humans: a test of how springs set stride frequency in bouncing gaits. *Journal of Applied Physiology, 71*(6), 2127-2132.

Farley, C. T., Blickhan, R., & Taylor, C. (1985). *Mechanics of human hopping- Model and experiments.* American Zoologist.

Farley, C. T., & Ferris, D. (1998). Biomechanics of walking and running: center of mass movements to muscle action. *Exercise and Sport Sciences Reviews, 26*, 253.

Farley, C. T., & Gonzalez, O. (1996). Leg stiffness and stride frequency in human running. *Journal of Biomechanics, 29*(2), 181-186.

Farley, C. T., Houdijk, H. H., Van Strien, C., & Louie, M. (1998). Mechanism of leg stiffness adjustment for hopping on surfaces of different stiffnesses. *Journal of Applied Physiology, 85*(3), 1044-1055.

Farley, C. T., & Morgenroth, D. C. (1999). Leg stiffness primarily depends on ankle stiffness during human hopping. *Journal of Biomechanics, 32*(3), 267-273.

Ferris, D. P., & Farley, C. T. (1997). Interaction of leg stiffness and surface stiffness during human hopping. *Journal of Applied Physiology*, *82*(1), 15-22.

Ferris, D. P., Liang, K., & Farley, C. T. (1999). Runners adjust leg stiffness for their first step on a new running surface. *Journal of Biomechanics, 32*(8), 787-794.

Ferris, D. P., Louie, M., & Farley, C. T. (1998). Running in the real world: adjusting leg stiffness for different surfaces. *Proceedings of the Royal Society of London B: Biological Sciences, 265*(1400), 989-994.

Fleming, P. (2011). Artificial turf systems for sport surfaces: current knowledge and research needs. *Proceedings of the Institution of Mechanical Engineers, Part P: Journal of Sports Engineering and Technology*, *225*(2), 43-63.

Floría, P., Sánchez-Sixto, A., Ferber, R., & Harrison, A. J. (2018). Effects of running experience on coordination and its variability in runners. *Journal of Sports Sciences, 36*(3), 272-278.

Fuller, C. W., Dick, R. W., Corlette, J., & Schmalz, R. (2007a). Comparison of the incidence, nature and cause of injuries sustained on grass and new generation artificial turf by male and female football players. Part 1: match injuries. *British Journal of Sports Medicine, 41*(suppl 1), i20-i26. doi:10.1136/bjsm.2007.037267

Fuller, C. W., Dick, R. W., Corlette, J., & Schmalz, R. (2007b). Comparison of the incidence, nature and cause of injuries sustained on grass and new generation artificial turf by male and female football players. Part 2: training injuries. *British Journal of Sports Medicine, 41*(suppl 1), i27-i32.

Gains, G. L., Swedenhjelm, A. N., Mayhew, J. L., Bird, H. M., & Houser, J. J. (2010). Comparison of speed and agility performance of college football players on field turf and natural grass. *The Journal of Strength & Conditioning Research, 24*(10), 2613-2617.

Glazier, P. S., Davids, K., & Bartlett, R. M. (2003). Dynamical systems theory: a relevant framework for performance-oriented sports biomechanics research. *Sportscience, 7*

Granata, K., Padua, D., & Wilson, S. (2002). Gender differences in active musculoskeletal stiffness. Part II. Quantification of leg stiffness during functional hopping tasks. *Journal of Electromyography and Kinesiology, 12*(2), 127-135.

Grimmer, S., Ernst, M., Günther, M., & Blickhan, R. (2008). Running on uneven ground: leg adjustment to vertical steps and self-stability. *Journal of Experimental Biology, 211*(18), 2989-3000.

Gutmann, A. K., & Bertram, J. E. (2017). Metabolic cost of human hopping. *Journal of Experimental Biology, 220*(9), 1654-1662.

Hamill, J., Haddad, J. M., Heiderscheit, B. C., Van Emmerik, R. E., & Li, L. (2006). Clinical relevance of variability in coordination. *Movement System Variability*, 153-165.

Hamill, J., Palmer, C., & Van Emmerik, R. E. (2012). Coordinative variability and overuse injury. *Sports Medicine, Arthroscopy, Rehabilitation, Therapy & Technology, 4*(1), p 45.

Hamill, J., van Emmerik, R. E., Heiderscheit, B. C., & Li, L. (1999). A dynamical systems approach to lower extremity running injuries. *Clinical Biomechanics, 14*(5), 297-308.

Hanavan Jr, E. P. (1964). A mathematical model of the human body. United States Aerospace Research Laboratories,Technical Report 62-102, 1-149.

Hein, T., Schmeltzpfenning, T., Krauss, I., Maiwald, C., Horstmann, T., & Grau, S. (2012). Using the variability of continuous relative phase as a measure to discriminate between healthy and injured runners. *Human Movement Science, 31*(3), 683-694.

Hennig, E. M., & Sterzing, T. (2010). The influence of soccer shoe design on playing performance: a series of biomechanical studies. *Footwear Science, 2*(1), 3-11.

Hobara, H., Inoue, K., Muraoka, T., Omuro, K., Sakamoto, M., & Kanosue, K. (2010). Leg stiffness adjustment for a range of hopping frequencies in humans. *Journal of Biomechanics, 43*(3), 506-511.

Hunter, I., & Smith, G. A. (2007). Preferred and optimal stride frequency, stiffness and economy: changes with fatigue during a 1-h high-intensity run. *European Journal of Applied Physiology, 100*(6), 653-661.

Karamanidis, K., Arampatzis, A., & Brüggemann, G.-P. (2006). Adaptational phenomena and mechanical responses during running: effect of surface, aging and task experience. *European Journal of Applied Physiology, 98*(3), 284-298.

Kerdok, A. E., Biewener, A. A., McMahon, T. A., Weyand, P. G., & Herr, H. M. (2002). Energetics and mechanics of human running on surfaces of different stiffnesses. *Journal of Applied Physiology, 92*(2), 469-478.

Komar, J., Seifert, L., & Thouvarecq, R. (2015). What Variability tells us about motor expertise: measurements and perspectives from a complex system approach. *Movement & Sport Sciences,* 3, 65-77.

Kuitunen, S., Ogiso, K., & Komi, P. (2011). Leg and joint stiffness in human hopping. *Scandinavian Journal of Medicine & Science in Sports, 21*(6), e159-e167.

Kulessa, D. J., Gollhofer, A., & Gehring, D. (2017). The influence of football shoe characteristics on athletic performance and injury risk–a review. *Footwear Science, 9*(1), 49-63.

Kurz, M. J., Stergiou, N., Buzzi, U. H., & Georgoulis, A. D. (2005). The effect of anterior cruciate ligament recontruction on lower extremity relative phase dynamics during walking and running. *Knee Surgery, Sports Traumatology, Arthroscopy, 13*(2), 107-115.

Lamb, P. F., & Stöckl, M. (2014). On the use of continuous relative phase: Review of current approaches and outline for a new standard. *Clinical Biomechanics, 29*(5), 484-493.

Latash, M. L., & Zatsiorsky, V. M. (1993). Joint stiffness: Myth or reality? *Human Movement Science, 12*(6), 653-692.

Mack, C. D., Hershman, E. B., Anderson, R. B., Coughlin, M. J., McNitt, A. S., Sendor, R. R., & Kent, R. W. (2018). Higher rates of lower extremity injury on synthetic turf compared with natural turf among national football league athletes: epidemiologic confirmation of a biomechanical hypothesis. *The American Journal of Sports Medicine,* 189–196.

Maquirriain, J. (2013). The interaction between the tennis court and the player: how does surface affect leg stiffness? *Sports Biomechanics, 12*(1), 48-53.

Marigold, D. S., & Patla, A. E. (2005). Adapting locomotion to different surface compliances: neuromuscular responses and changes in movement dynamics. *Journal of Neurophysiology, 94*(3), 1733-1750.

McMahon, T. A., & Cheng, G. C. (1990). The mechanics of running: how does stiffness couple with speed? *Journal of Biomechanics, 23,* 65-78.

McMahon, T. A., & Greene, P. R. (1979). The influence of track compliance on running. *Journal of Biomechanics, 12*(12), 893-904.

Meijer, K., Dethmers, J., Savelberg, H. H., Willems, P., & Wijers, B. (2007). The influence of third generation artificial soccer turf characteristics on ground reaction forces during running. *ISBS-Conference Proceedings Archive*

Meyers, M. C. (2013). Incidence, mechanisms, and severity of match-related collegiate women's soccer injuries on FieldTurf and natural grass surfaces: a 5-year prospective study. *The American Journal of Sports Medicine, 41*(10), 2409-2420.

Meyers, M. C. (2017). Incidence, Mechanisms, and Severity of Match-Related Collegiate Men's Soccer Injuries on FieldTurf and Natural Grass Surfaces: A 6-Year Prospective Study. *The American Journal of Sports Medicine, 45*(3), 708-718.

Miller, R. H., Chang, R., Baird, J. L., Van Emmerik, R. E., & Hamill, J. (2010). Variability in kinematic coupling assessed by vector coding and continuous relative phase. *Journal of Biomechanics, 43*(13), 2554-2560.

Miller, R. H., Meardon, S. A., Derrick, T. R., & Gillette, J. C. (2008). Continuous relative phase variability during an exhaustive run in runners with a history of iliotibial band syndrome. *Journal of Applied Biomechanics, 24*(3), 262-270.

Millett, E. L., Moresi, M. P., Watsford, M. L., Taylor, P. G., & Greene, D. A. (2018). Variations in lower body stiffness during sports-specific tasks in well-trained female athletes. *Sports Biomechanics*, 1-16.

Morin, J.-B. (2018). A Simple Method for Measuring Lower Limb Stiffness During Running *Biomechanics of Training and Testing* (pp. 165-193): Springer.

Moritz, C. T., & Farley, C. T. (2004). Passive dynamics change leg mechanics for an unexpected surface during human hopping. *Journal of Applied Physiology, 97*(4), 1313-1322.

Mudie, K. L., Gupta, A., Green, S., Hobara, H., & Clothier, P. J. (2017). A comparison of vertical stiffness values calculated from different measures of center of mass displacement in single-leg hopping. *Journal of Applied Biomechanics, 33*(1), 39-47.

Müller, C., Sterzing, T., Lake, M., & Milani, T. L. (2010). Different stud configurations cause movement adaptations during a soccer turning movement. *Footwear Science, 2*(1), 21-28.

Müller, C., Sterzing, T., Lange, J., & Milani, T. L. (2010). Comprehensive evaluation of player-surface interaction on artificial soccer turf. *Sports Biomechanics, 9*(3), 193-205.

Müller, R., Grimmer, S., & Blickhan, R. (2010). Running on uneven ground: leg adjustments by muscle pre-activation control. *Human Movement Science, 29*(2), 299-310.

Nematollahi, M., Razeghi, M., Mehdizadeh, S., Tabatabaee, H., Piroozi, S., Shirazi, Z. R., & Rafiee, A. (2016). Inter-Segmental Coordination Pattern in Patients with Anterior Cruciate Ligament Deficiency during a Single-Step Descent. *PloS one, 11*(2), e0149837.

Newell, K. (1985). Coordination, control and skill *Advances in Psychology* (Vol. 27, 295-317): Elsevier.

Newell, K. (1986). Constraints on the development of coordination. *Motor Development in Children: Aspects of Coordination and Control*

Nigg, B. M., & Yeadon, M. (1987). Biomechanical aspects of playing surfaces. *Journal of Sports Sciences, 5*(2), 117-145.

Noghondar, F. A., & Yazdi, N. K. (2017). Assessment of patterns and variability in lower extremity coordination between genders with different shoe insole stiffness during jump-landing tasks. *Human Movement, 18*(1), 37-43.

Novacheck, T. F. (1998). The biomechanics of running. *Gait & Posture, 7*(1), 77-95.

Padua, D. A., Arnold, B. L., Perrin, D. H., Gansneder, B. M., Carcia, C. R., & Granata, K. P. (2006). Fatigue, vertical leg stiffness, and stiffness control strategies in males and females. *Journal of Athletic Training, 41*(3), p 294.

Padulo, J., Chamari, K., & Ardigò, L. P. (2014). Walking and running on treadmill: the standard criteria for kinematics studies. *Muscles, Ligaments and Tendons Journal, 4*(2), p 159.

Peters, B. T., Haddad, J. M., Heiderscheit, B. C., Van Emmerik, R. E., & Hamill, J. (2003). Limitations in the use and interpretation of continuous relative phase. *Journal of Biomechanics, 36*(2), 271-274.

Pickering Rodriguez, E. C., Watsford, M. L., Bower, R. G., & Murphy, A. J. (2017). The relationship between lower body stiffness and injury incidence in female netballers. *Sports Biomechanics*, *16*(3), 361-373. doi:10.1080/14763141.2017.1319970

Prejean, B. J., & Ricard, M. D. (2019). A quantification of lower-limb coordinative variability during running with different levels of midsole cushioning. *Footwear Science*, *11*(2), 93-104.

Pruyn, E. C., Watsford, M., & Murphy, A. (2014). The relationship between lower-body stiffness and dynamic performance. *Applied Physiology, Nutrition, and Metabolism*, *39*(10), 1144-1150.

Pupo, J. D., Dias, J. A., Gheller, R. G., Detanico, D., & Santos, S. G. D. (2013). Stiffness, intralimb coordination, and joint modulation during a continuous vertical jump test. *Sports Biomechanics, 12*(3), 259-271.

Raffalt, P. C., Alkjær, T., & Simonsen, E. B. 2016). Intra-and inter-subject variation in lower limb coordination during countermovement jumps in children and adults. *Human Movement Science, 46*, 63-77.

Ranavolo, A., Don, R., Cacchio, A., Serrao, M., Paoloni, M., Mangone, M., & Santilli, V. (2008). Comparison between kinematic and kinetic methods for computing the vertical displacement of the center of mass during human hopping at different frequencies. *Journal of Applied Biomechanics*, *24*(3), 271-279.

Reenalda, J., Maartens, E., Buurke, J. H., & Gruber, A. H. (2019). Kinematics and shock attenuation during a prolonged run on the athletic track as measured with inertial magnetic measurement units. *Gait & Posture, 68*, 155-160.

Reenalda, J., Maartens, E., Homan, L., & Buurke, J. J. (2016). Continuous three dimensional analysis of running mechanics during a marathon by means of inertial magnetic measurement units to objectify changes in running mechanics. *Journal of Biomechanics, 49*(14), 3362-3367.

Rennie, D. J., Vanrenterghem, J., Littlewood, M., & Drust, B. (2016). Can the natural turf pitch be viewed as a risk factor for injury within Association Football? *Journal of Science and Medicine in Sport, 19*(7), 547-552.

Riley, M. A., & Turvey, M. T. (2002). Variability and determinism in motor behavior. *Journal of Motor Behavior, 34*(2), 99-125.

Rosalie, S. M., & Müller, S. (2012). A model for the transfer of perceptual-motor skill learning in human behaviors. *Research Quarterly for Exercise and Sport*, *83*(3), 413-421.

Sabatini, A. M., Martelloni, C., Scapellato, S., & Cavallo, F. (2005). Assessment of walking features from foot inertial sensing. *IEEE Transactions on Biomedical Engineering, 52*(3), 486-494.

Saini, M., Kerrigan, D., Thirunarayan, M., & Duff-Raffaele, M. (1998). The vertical displacement of the center of mass during walking: a comparison of four measurement methods. *Journal of biomechanical engineering, 120*(1), 133-139.

Sánchez, C. C., Moreno, F. J., Vaíllo, R. R., Romero, A. R., Coves, Á., & Murillo, D. B. (2017). The role of motor variability in motor control and learning depends on the nature of the task and the individual's capabilities. *European Journal of Human Movement, 38*, 12-26.

Schepers, H., Giuberti, M., & Bellusci, G. (2018). Xsens MVN: Consistent Tracking of Human Motion Using Inertial Sensing. *Xsens Technologies* (pp. 1-8).

Schrier, N. M., Wannop, J. W., Lewinson, R. T., Worobets, J., & Stefanyshyn, D. (2014). Shoe traction and surface compliance affect performance of soccer-related movements. *Footwear Science, 6*(2), 69-80.

Seay, J. F., Van Emmerik, R. E., & Hamill, J. (2011). Low back pain status affects pelvis-trunk coordination and variability during walking and running. *Clinical Biomechanics, 26*(6), 572-578.

Seifert, L., Button, C., & Davids, K. (2013). Key properties of expert movement systems in sport. *Sports Medicine, 43*(3), 167-178.

Seifert, L., Komar, J., Crettenand, F., & Millet, G. (2014). Coordination pattern adaptability: energy cost of degenerate behaviors. *PloS One, 9*(9), e107839.

Serpell, B. G., Ball, N. B., Scarvell, J. M., & Smith, P. N. (2012). A review of models of vertical, leg, and knee stiffness in adults for running, jumping or hopping tasks. *Journal of Sports Sciences, 30*(13), 1347-1363.

Severn, K. A., Fleming, P. R., & Dixon, N. (2008). The science of sports surface interactions for synthetic turf surfaces. *7th International Conference on the Engineering of Sport, Biarritz, France*

Silva, D. C., Santos, R., Vilas-Boas, J. P., Macedo, R., Montes, A., & Sousa, A. S. (2017). The influence of different soccer cleat type on kinetic, kinematic and neuromuscular ankle variables in artificial turf. *Footwear Science, 9*(1), 21-31.

Slawinski, J., Heubert, R., Quievre, J., Billat, V., & Hannon, C. (2008). Changes in spring-mass model parameters and energy cost during track running to exhaustion. *The Journal of Strength & Conditioning Research, 22*(3), 930-936.

Smallmana, C. L. W., Graham, R. B., & Stevenson, J. M. (2013). The effect of an on-body assistive device on transverse plane trunk coordination during a load carriage task. [Article]. *Journal of Biomechanics, 46*(15), 2688-2694. doi:10.1016/j.jbiomech.2013.07.034

Stergiou, N., & Decker, L. M. (2011). Human movement variability, nonlinear dynamics, and pathology: is there a connection? *Human Movement Science, 30*(5), 869-888.

Stergiou, N., Jensen, J. L., Bates, B. T., Scholten, S. D., & Tzetzis, G. (2001). A dynamical systems investigation of lower extremity coordination during running over obstacles. *Clinical Biomechanics, 16*(3), 213-221.

Strohrmann, C., Harms, H., Kappeler-Setz, C., & Troster, G. (2012). Monitoring kinematic changes with fatigue in running using body-worn sensors. *IEEE Transactions on Information Technology in Biomedicine, 16*(5), 983-990.

van Emmerik, R. E., Ducharme, S. W., Amado, A. C., & Hamill, J. (2016). Comparing dynamical systems concepts and techniques for biomechanical analysis. *Journal of Sport and Health Science, 5*(1), 3-13.

Waxman, J. P., Ford, K. R., Nguyen, A.-D., & Taylor, J. B. (2018). Female Athletes With Varying Levels of Vertical Stiffness Display Kinematic and Kinetic Differences During Single-Leg Hopping. *Journal of Applied Biomechanics, 34*(1), 65-75.

Williams, A. M., Davids, K., & Williams, J. G. P. (1999). *Visual perception and action in sport*: Taylor & Francis.

Williams III, D. B., Davis, I. M., Scholz, J. P., Hamill, J., & Buchanan, T. S. (2004). High-arched runners exhibit increased leg stiffness compared to low-arched runners. *Gait & Posture, 19*(3), 263-269.

Williams III, D. B., McClay, I. S., & Hamill, J. (2001). Arch structure and injury patterns in runners. *Clinical Biomechanics, 16*(4), 341-347.

Williams III, D. B., Murray, N. G., & Powell, D. W. (2016). Athletes who train on unstable compared to stable surfaces exhibit unique postural control strategies in response to balance perturbations. *Journal of Sport and Health Science, 5*(1), 70-76.

Williams, S., Hume, P. A., & Kara, S. (2011). A review of football injuries on third and fourth generation artificial turfs compared with natural turf. *Sports Medicine, 41*(11), 903-923.

Wilson, A., & Lichtwark, G. (2011). The anatomical arrangement of muscle and tendon enhances limb versatility and locomotor performance. *Philosophical Transactions of the Royal Society B: Biological Sciences, 366*(1570), 1540-1553.

Winter, D. A. (2009). *Biomechanics and motor control of human movement*: John Wiley & Sons.

Xsens Technologies. MTw Awinda User Manual. Document MV0319P, Revision X, Oct 2018.

APPENDIX

Appendix A

According to Dalleau et al. (2004) and Morin et al. (2005), the sine wave method of estimating peak vertical ground reaction force assumes that the vertical ground reaction force signal plotted as a function of time [$GRF_{vert}(t)$] would resemble a sine wave curve that can be model using the following equation:

$$GRF_{vert}(t) = peakGRF_{vert} \cdot sin\left(\frac{\pi}{T_c} \cdot t\right) \qquad \text{(A4)}$$

where *peak* GRF_{vert} is peak vertical ground reaction force and T_c is contact time.

To solve for *peak* GRF_{vert}, the change in momentum during the contact phase must be considered using the following equation:

$$\int_0^{T_c}[GRF_{vert}(t) - m \cdot g] \cdot dt = m \cdot \Delta v = m \cdot g \cdot T_f \qquad \text{(A5)}$$

where *m* is the mass of the body, *g* is gravitational acceleration, *v* is the vertical velocity, and T_f is flight time.

By substituting $GRF_{vert}(t)$ in Equation A5 with Equation A4, we get the following:

$$\int_0^{T_c}\left[peakGRF_{vert} \cdot sin\left(\frac{\pi}{T_c} \cdot t\right) - m \cdot g\right] \cdot dt = m \cdot \Delta v = m \cdot g \cdot T_f \qquad \text{(A6)}$$

which reduces to:

$$\left\lfloor -peakGRF_{vert} \cdot \frac{T_c}{\pi} \cdot \cos\left(\frac{\pi}{T_c} \cdot t\right) \right\rfloor_0^{T_c} - m \cdot g \cdot T_c = m \cdot g \cdot T_f \tag{A7}$$

$$2 \cdot peakGRF_{vert} \cdot \frac{T_c}{\pi} = m \cdot g \cdot \left(T_f + T_c\right) \tag{A8}$$

Ultimately, this process results in the follow equation for estimating *peak GRF*$_{vert}$:

$$peakGRF_{vert} = m \cdot g \cdot \frac{\pi}{T_c} \cdot \left(\frac{T_f}{T_c} + 1\right) \tag{1}$$